ACADÉMIE DES SCIENCES
INSTITUT DE FRANCE

Comptes Rendus

Géoscience
Sciences de la Planète

Bruno Scalabrino, Yves Lagabrielle and Claudio Faccenna

Subduction of active spreading ridges and the disappearance of Andean-type cordilleras

CENTRE
MERSENNE

Research article

Geodynamics of continents and oceans - A tribute to Jean Aubouin

Subduction of active spreading ridges and the disappearance of Andean-type cordilleras

Bruno Scalabrino [*, a], **Yves Lagabrielle** [b] **and Claudio Faccenna** [c, d]

[a] Université Côte d'Azur, CNRS, Observatoire de la Côte d'Azur, IRD, Géoazur, 250 rue Albert Einstein, Sophia Antipolis 06560 Valbonne, France

[b] 35 Allée du Pargo, 56000 Vannes, France

[c] Departement of Science, Roma Tre University, Roma, Italy

[d] GFZ, German Research Center for Geoscience, Germany

E-mails: bruno.scalabrino@geoazur.unice.fr (B. Scalabrino), yveslagabrielle@yahoo.fr (Y. Lagabrielle), faccenna@uniroma3.it, claudio.faccenna@gfz-potsdam.de (C. Faccenna)

Abstract. We address the possible link between the age of subducting oceanic lithosphere and growth of elevated cordilleras versus extension-dominated arc regions. Singularity exists in South America: the lowest elevated Andean segments are found in Patagonia where the active Chile Ridge enters the trench. Subduction of active ridge triggers thermal doming, crustal extension and attenuation of former cordilleras. At the Antarctica–South America connection, three active ridge subductions induced the disruption of a former continuous cordillera during the opening of Drake Passage. Active ridge subduction induces lithosphere thermal erosion and related crustal extension in the upper plate. Evolution of regions worldwide experiencing ridge subduction confirms this hypothesis.

1. Introduction

Subduction of oceanic lithosphere beneath continental lithosphere is able to generate high relief cordilleras, such as the Andean belt in South America and the Sierra Nevada, Coastal Ranges, Rocky Mountains and Alaska Mountains in Northern America. However, with along many subduction zones worldwide, the continental lithosphere overriding the subducting oceanic lithosphere does not carry

high elevation belts. This is well observed for example, along the subduction zones of Alaska Peninsula, Aleutian Islands, Kuril Islands and Ryukyu Islands as well as along the overall Indonesia convergent boundary.

Explanations for such contrasting styles of the continental lithosphere overriding subducting oceanic lithosphere have long been proposed but are still a matter of debate. Classifications based on various characteristics describing the behaviour of the upper and lower plates suffer many exceptions [Shemenda, 1992, 1994, Uyeda, 1982, Uyeda and Kanamori, 1979]. At a global scale, differences
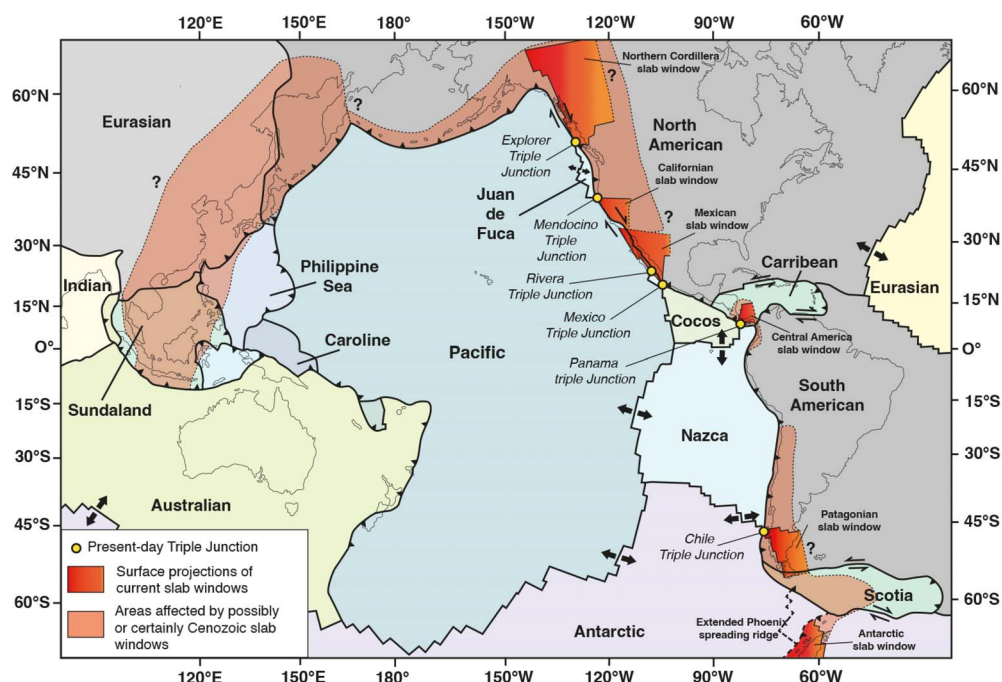
---

[*]Corresponding author

Figure 1. Present-day slab windows and probable location of areas affected by Cenozoic slab windows beneath SE Asia to Antarctica Peninsula [Dickinson and Snyder, 1979, Johnston and Thorkelson, 1997, Gorring and Kay, 2001, Sisson et al., 2003, Madsen et al., 2006, Breitsprecher and Thorkelson, 2009, Whittaker et al., 2007, Thorkelson et al., 2011, Müller et al., 2008, 2016 for predicted SE Asian slab window].

of topography between western and eastern Pacific cordilleras can be assigned as a function of subduction polarity, related slab retreat/advance and force balance [Doglioni et al., 1999, 2007]. For Vanderhaeghe and Duchêne [2010], the topography of the overriding plate is the consequence of the crust-lithospheric mantle ratio resulting from the interaction between slab kinematics and the degree of crust-mantle coupling/decoupling. Moreover, by looking at the force balance, mechanisms involving mantle drag beneath the upper plate can represent a prime role to the deformational regime at subduction zones [e.g. Husson, 2012]. Another point of view is to attempt to correlate simple parameters. For example, correlating the topography of the continent at a given active margin boundary with the age of the corresponding subducting oceanic lithosphere provide contrasted results [Garfunkel et al., 1986, Heuret and Lallemand, 2005, Heuret et al., 2011, Jarrard, 1986, Sdrolias and Müller, 2006]. In addition, lateral changes of rheology due to progressive variations in

the age of the subducting lithosphere are difficult to integrate into analogic or numerical experiments [DeLong et al., 1979, DeLong and Fox, 1977, Groome and Thorkelson, 2009, Uehara and Aoya, 2005]. More specifically, the situations involving the subduction of active spreading ridges leading to the opening of an asthenospheric slab window beneath a continental margin, although studied in detail [Thorkelson, 1996, Thorkelson and Taylor, 1989], have not been integrated into a model depicting the complete evolution of subduction cordilleras.

The purpose of this article is to examine the role played by the subduction of active spreading ridges on the evolution of subduction belts, with a focus on the processes leading to the attenuation and disappearance of the cordillera reliefs (Figure 1). We first discuss correlations between two parameters which may simply describe ocean-continent subduction zones. For a given transect across a subduction zone, these parameters are: (1) the mean elevation of the continent of the upper plate and, (2) the age of the

subducting oceanic lithosphere at trench. We point to a major singularity arising when considering this simple correlation at the global scale on one hand, and at a more regional scale, on the other hand.

Resolving this singularity at the scale of the Andean belt leads us to emphasize the role played by the subduction of active spreading ridges and the opening of slab windows in the progressive decrease of the elevation and volume of the cordillera. We finally test the idea that a causal link exists between lowering and disappearance of subduction cordilleras reliefs and opening of slab windows due to spreading ridge subduction by discussing a number of situations worldwide.

2. Correlating the cordillera topography with the age of the subducting oceanic lithosphere: the singularity

At the scale of the entire peri-Pacific subduction boundaries, there is a negative correlation between the elevation of the continental crust over the subducting oceanic lithosphere (corresponding to the forearc to the back-arc region) and the age of the oceanic lithosphere at the trench for a given transect (blue dotted line with a correlation coefficient $R^2 = -0.16$, Figure 2). Without considering transects located close to modern subducting spreading ridges, low elevation subduction belts are found in the west Pacific regions where the descending lithosphere is of Mesozoic age (Figure 2). High elevation cordilleras such as the Andes, the Western American Cordillera and the Alaska belt, are found along the eastern Pacific regions where the subducting lithosphere is Cenozoic in age (Figure 2). However, at a more regional scale, when considering the relations between the elevation of the Andean crust and the age of the oceanic lithosphere at the trench, the negative correlation is changed into a positive correlation (red dotted line with a correlation coefficient $R^2 = 0.59$ on Figures 2, and 3). This constitutes a singularity that needs to be solved. Indeed, the highest and widest elevation of the Andes, corresponding to the Altiplano-Puna region, occurs where the oceanic lithosphere is the oldest (Eo-Oligocene) (transects S15 and S16 Figures 2 and 3) and by contrast, the lowermost segments of the Cordillera, in Central Patagonia, occur at the site of the Chile Triple junction (CTJ), where the oceanic lithosphere is zero Ma

in age, that is where the Chile spreading ridge enters the trench (transect S19 Figures 2 and 3). Southward of the CTJ, the Andes disappear completely into the ocean due to the opening of the Scotia Sea during the Neogene [Eagles, 2003, Eagles et al., 2005, 2006, Lagabrielle et al., 2009, Livermore et al., 2005, 2007]. This occurred following a period of rifting that affected the Antarctica–South America connection where a high subduction cordillera existed [Eagles and Jokat, 2014, Ghiglione and Ramos, 2005, Ghiglione et al., 2016, Kraemer, 2003, Vérard et al., 2012]. In the following section, we will show that the attenuation and complete disruption of this former Cordillera occurred in relation with the subduction of several active spreading ridges.

3. Resolving the singularity along the Andean Cordillera

At present, the Andes are actively growing in the regions north of the Chile Triple Junction and south of the Cocos–Nazca–Mid-America trench junction [e.g. Allmendinger et al., 1997, Gregory-Wodzicki, 2000, Isacks, 1988, Jordan et al., 1983, Ramos, 1989]. Active eastward verging thrusts develop in the frontal regions of the Andes where the Amazonian lithosphere is underthrust beneath the Andean lithosphere [Taboada et al., 2000]. The resulting continental plateau, formed in response to the initiation of westward South America continental (or Amazonian block) collision, stretches for North–South 1800 km-long and attains a width of 350–400 km. Westward verging thrusts also develop in the western Andean belt [Armijo et al., 2015]. Current uplift occurs with the highest values recorded in the central Andes, in the Altiplano-Puna regions [e.g. Gregory-Wodzicki, 2000, Husson and Sempere, 2003, Perkins et al., 2016]. The Altiplano-Puna Andean plateau was uplifted primarily because of crustal thickening produced by horizontal shortening of a thermally softened lithosphere [e.g. Allmendinger et al., 1997, Gerbault et al., 2005] with a recent evolution linked to gravity-driven crustal channel [Husson and Sempere, 2003]. Uplift in the region of the Altiplano began around 25 Ma, coincident with increased convergence rate and inferred shallowing of subduction; uplift in the Puna commenced 5–10 million years later [Sempere et al., 1990, Allmendinger et al., 1997, Charrier et al., 2013]. Therefore, the current
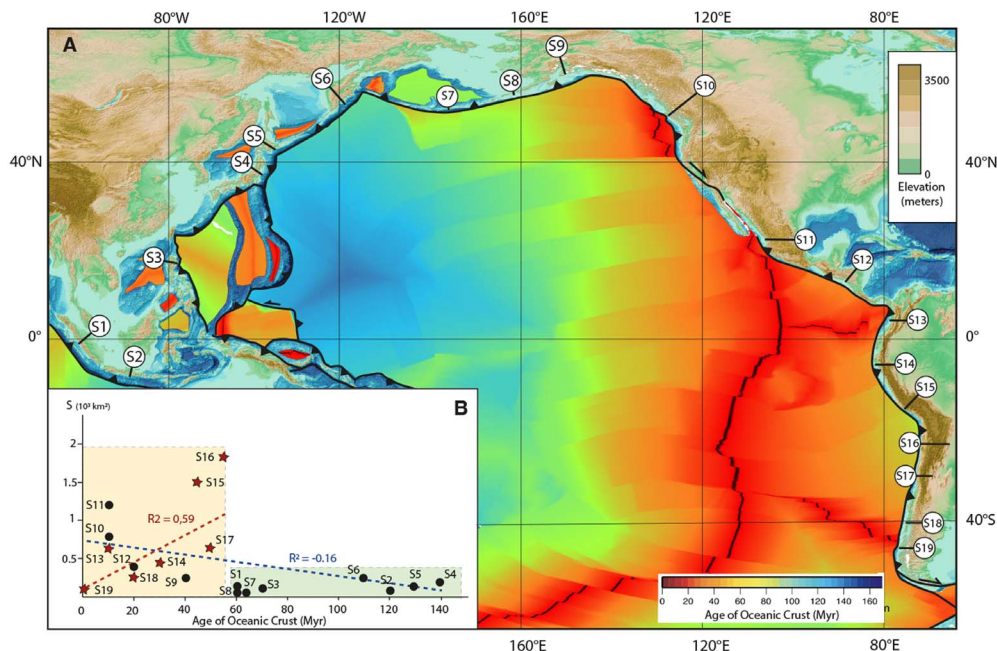
Figure 2. (A) Peri-Pacific overview showing continental topography (Digital Elevation Model, GTOPO30) and age of the oceanic lithosphere [from Seton et al., 2020]. 19 transects were selected from Indonesia to southern South America. Max/mean/min topographic profiles of each 19 transects were extracted and are available on Supplementary files. (B) Correlations between age of the oceanic lithosphere at trench and the surface area S of the overriding plate domain along the 19 selected transects. The surface area S was extracted from mean elevation of the 19 selected transects from peri-Pacific region (using the midpoint Reimann Sums method). Surface area of transects across the Andean Cordillera are represented with red stars. Green (from west Pacific to Aleutian regions) and orange (east Pacific regions) boxes represent the peri-pacific correlations between topography and age of the oceanic lithosphere. The blue dotted line corresponds to the negative correlation observed along the peri-Pacific regions with a correlation coefficient $R^2 = -0.16$. The red dotted line corresponds to the positive correlation described between the Andean Cordillera topography and the age of the subducted oceanic lithosphere at trench. The correlation coefficient $R^2 = 0.56$ was calculated using red stars.

topography of South America is a recent feature and contrasted morphological changes have occurred along various segments of the Andean cordillera during the last 50 Ma.

An overview of the average evolution of the topography of the Andean orogen highlights that an important decrease of max and mean elevation occurs starting from 35° S (Figure 3). At the site of the present-day Chile Triple Junction, the mean topography of the Andean belt is reduced. Here, the cordillera lacks central high relief and the average elevation reaches a few hundred meters [Figure 3 and see Scalabrino et al., 2010 for more details]. It is demonstrated that the uplift of the Central Patag-

onia Cordillera occurred from 25 to 15 Ma in response to compressional deformation of the arc domain [Blisniuk et al., 2005, Lagabrielle et al., 2004, Ramos, 1989, Thomson et al., 2001]. Eastward verging frontal thrusts bring the external units of the Cordillera over molasse deposits of the Pampa regions (Figure 4A). After this period linked to the break-up of the Farallon plate [Londsale, 2005] inducing the acceleration rate of the subduction of the Nazca plate [Somoza, 1998, Pardo-Casas and Molnar, 1987], the interval 16–14 Ma was characterized by the tip of a long segment of the SCR entering the Chile trench at around 55° S [Cande and Leslie, 1986]. In the Patagonian Cordillera, the compression
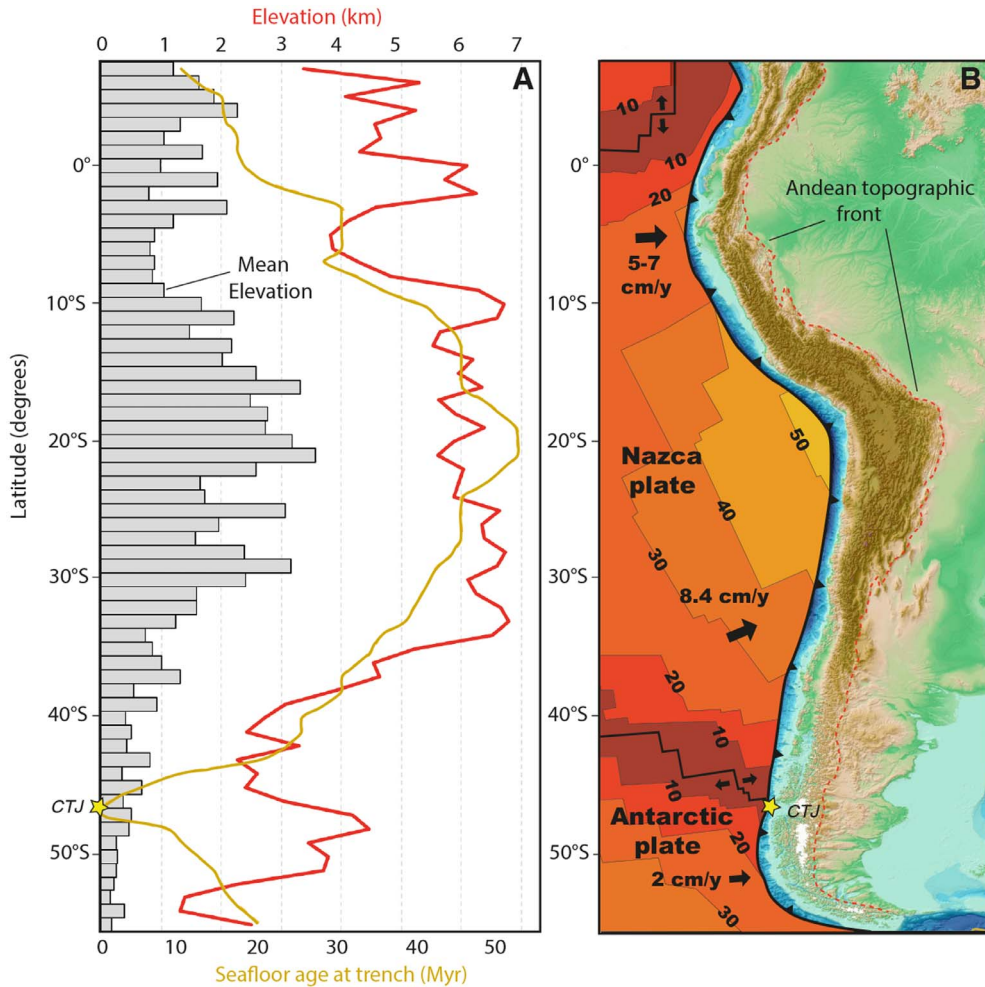
Figure 3. The positive correlation between the Andean topography and the age of the oceanic lithosphere at trench. (A) Maximum (red line) and mean (gray area) elevations of the Andean Cordillera in 1° latitude bins (with 100-km width). Yellow line represents the seafloor age (Myr). The location of the Chile Triple Junction (CTJ) corresponds to the yellow star. (B) Andean topography (Digital Elevation Model, GTOPO30) and seafloor age [from Seton et al., 2020, Sdrolias and Müller, 2006]. The trench is represented by thick line with triangles. Red dotted line limits the Andean topographic front [from Horton, 2018]. Relative plate velocities from DeMets et al. [1990].

resumed and a major phase of erosion resulted to the rapid peneplanation of the eastern side of the frontal belt (Figure 4B). To the west, low-temperature thermochronology studies show that the late Cretaceous topographic evolution of the Cordillera was governed by complex feedbacks between deep geodynamic processes [Georgieva et al., 2019, Guillaume et al., 2013] with climate [Thomson et al., 2010, Willett et al., 2020], transcurrent deformation along the dex-

tral strike-slip Liquiñe-Ofqui Fault Zone (LOFZ) [e.g. Cembrano et al., 2002] and upper crustal shortening along NW–SE thrusts related to the LOFZ [Georgieva et al., 2016, Stevens Godard and Fosdick, 2019]. The occurrence of remnants of glacial deposits and landform perched surfaces preserved in the central and eastern parts of the cordillera also suggests higher elevations at this time [Lagabrielle et al., 2010, Scalabrino et al., 2010, 2011].
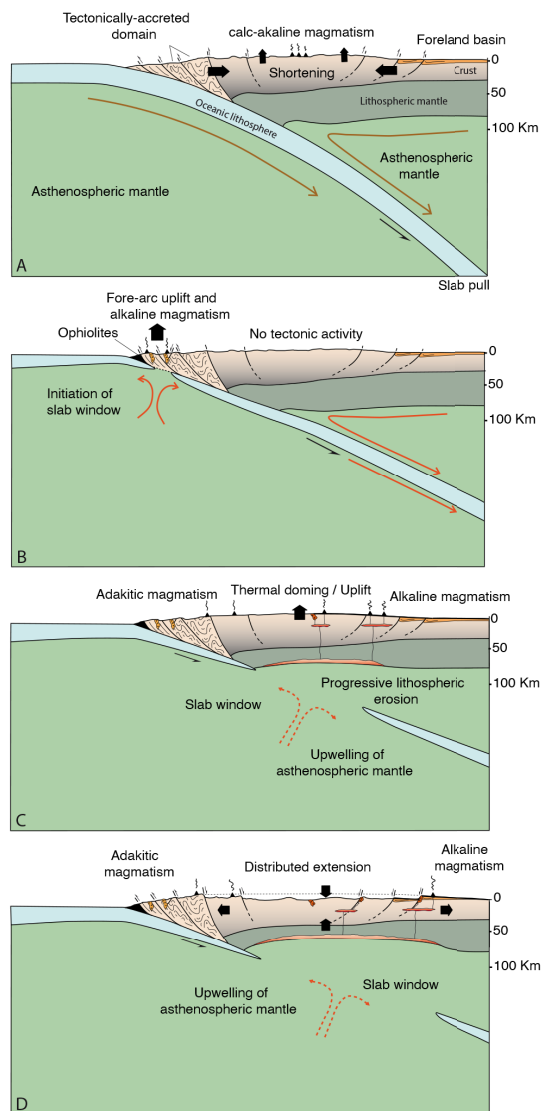
Figure 4. Lithospheric-scale model of circum-Pacific cordilleras evolution during active spreading ridge subduction from a "classical cold" subduction stage (A) to a "hot" subduction stage (B–D). After a compressional stage linked to arrival of high bathymetric features close to the trench (A), regional thermal uplift, or related-uplift dynamic topography, represents the first impact of uprising of hot asthenosphere flows through the slab-window (B–C). Extensional to transtensional deformation associated with variability of magmatism comprising voluminous OIB intraplate activities substantiates the thermal erosion and the weakening of the continental lithosphere above and around slab window pathways (D).

From 15 to 3 Ma, large alkaline plateau basalts were erupted in the eastern Patagonia Cordillera (Figure 4C) [Espinoza et al., 2008, Gorring et al., 1997, 2003, Ramos and Kay, 1992]. These major magmatic events are likely linked to the development of a tear in the Nazca slab [Guivel et al., 2006], followed by the development of the Patagonian slab window [Gorring and Kay, 2001, Bourgois and Michaud, 2002, Breitsprecher and Thorkelson, 2009, Espinoza et al., 2010, Lagabrielle et al., 2004, Russo et al., 2010]. During this period, no significant tectonic and arc magmatic activities are known in the cordillera domain, but the overall elevation of the cordillera remained high south of CTJ (Figure 4C). As depicted in Figure 4C, Scalabrino et al. [2010] suggest that synchronously to alkaline magmatism, thermal uplift was able to maintain high elevation plateau, creating conditions for major eastward glaciers dynamics as shown by 7 Ma to 3 Ma till deposits interbedded with alkaline lavas [Lagabrielle et al., 2010, Mercer and Sutter, 1982]. Thermal doming, or dynamic topography according to some authors, is interpreted as the first consequence of the presence of hot materiel beneath the upper plate [Ávila and Dávila, 2018, 2020, Guillaume et al., 2009, Scalabrino et al., 2010].

The cessation of the tectonic activity along the Patagonian Cordillera coincides with the collision and subduction of the Chile Spreading Ridge, which started at 14 Ma at the site of the present-day Tierra de Fuego. Negative tectonic inversion of the front of the Cordillera occurred recently in Central Patagonia as a response to the presence of very young subducted segments of the Chile Ridge buried at depth [Scalabrino et al., 2010, 2011]. This frontal inversion is accompanied by the subsidence of internal asymmetrical basins limited by normal faults, inside the cordillera itself (Figure 4D). According to Scalabrino et al. [2010, 2011], extensional tectonics play an important role in the attenuation of the reliefs of the cordillera (Figure 4D). Extension was triggered by the presence of hot mantle belonging to the subducted Chile Ridge lithosphere moving eastward beneath the southern tip of the South America Plate.

South of the present-day Chile Triple Junction, geological studies revealed that the Andean Cordillera started growing in earliest Cenozoic times, that is well before the current Central Cordillera of Chile–Peru–Bolivia which was at that time with elevations close to sea-level (Figure 5A) [e.g. Armijo et al., 2015,
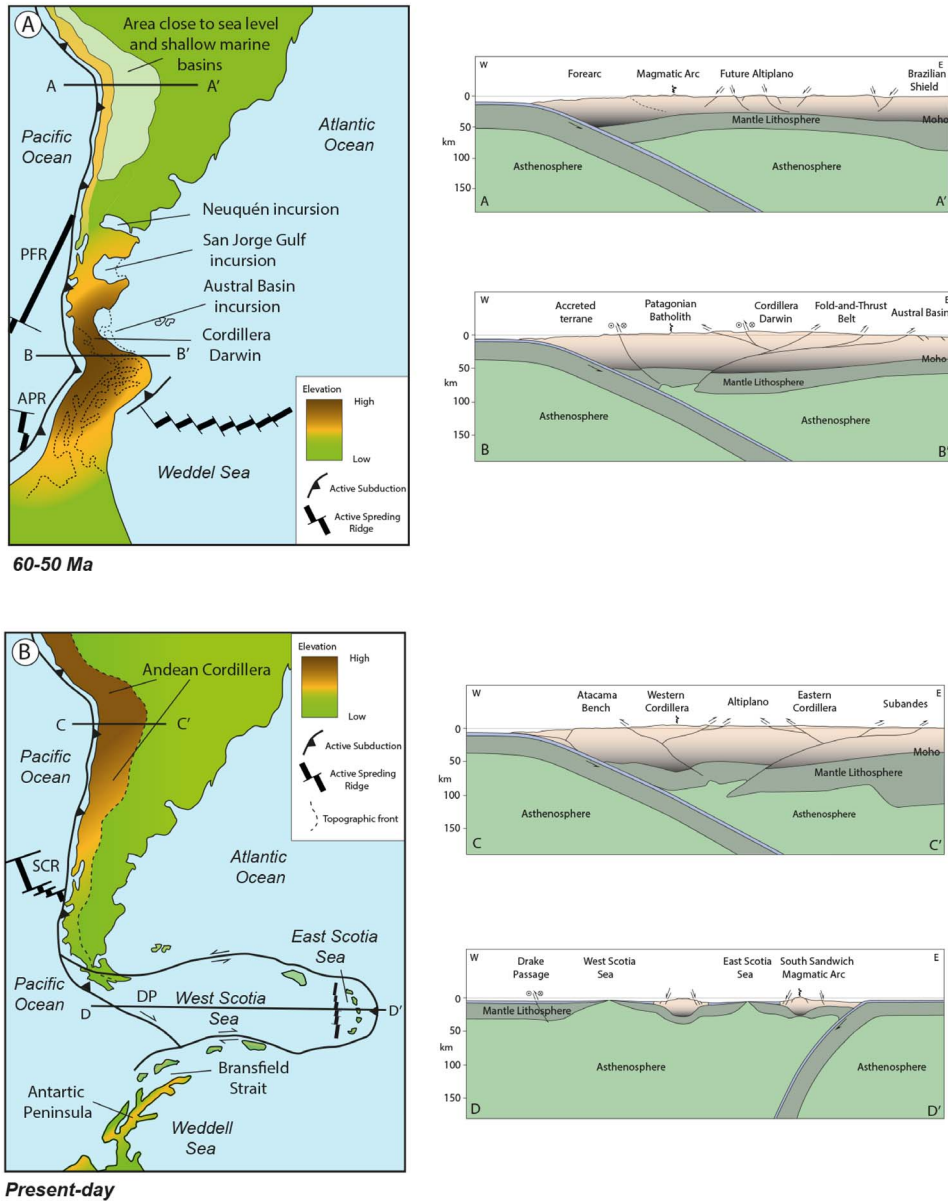
Figure 5. Early Tertiary (A) and present-day (B) configurations of the South American plate and West Antarctica Peninsula. (A) Paleoelevation of South American plate and supposed continental connection to the West Antarctica Peninsula at 60–50 Ma [from Boschman, 2021, Ghiglione, 2016, Reguero et al., 2013, Riley et al., 2023]. Cross section A–A′ represents the large-scale 2D structure of the Andean magmatic arc and back-arc domains [simplified from Armijo et al., 2015] and the cross-section B–B′ is a proposed structural view of the former elevated Cordillera (including the Cordillera Darwin) connecting the South American plate to the West Antarctica Peninsula [after Cunningham, 1993, 1995, Ghiglione, 2016, Ghiglione et al., 2016, Ronda et al., 2019]. (B) Present-day elevation of the Andean and the West Antarctica Peninsula. Cross section C–C′ corresponds to the actual tectonic structure of the Andean belt at 21° S [after Armijo et al., 2015], cross section D–D′ illustrates the present-day setting of the Drake Passage and Scotia Sea back-arcs domains.

Boschman, 2021, Gregory-Wodzicki, 2000, Horton, 2005, Jordon et al., 2010, Lamb et al., 1997, Sempere et al., 1997]. Exhumation of the internal part of the Cordillera Darwin in Tierra del Fuego initiated during the Eocene, indicating that there was a larger cordillera belt at the site of the current tip of southernmost South America (Figure 5A) [Coutand et al., 1999, Cunningham, 1993, 1995, Fosdick et al., 2011, Ghiglione et al., 2016, Müller et al., 2021, Ronda et al., 2019]. At present, the Central Andean Cordillera regions expose highest elevation and the widest belt (Figure 5B), while to the south, remnants of the former Southern Andean Cordillera form restricted parts of the end of South America continent and are still exposed along the Antarctic Peninsula (Figure 5B). Plate reconstructions of the South America–Antarctica region involve frequent interplay between ocean lithosphere subduction and accretion at young spreading centers since Mesozoic times. Based on a compilation of various regional kinematics models gathered from the literature, Figure 6 shows the evolution of the interactions between trenches and ridges to the south of South America. The current Drake Passage area was the site of the subduction of at least three active spreading ridges (Figure 6) and its mantle is now characterized by a strong thermal anomaly. Tomography models reveal a zone of strongly attenuated P and S waves extending from the CTJ to the Antarctica Peninsula [e.g. Ben Mansour et al., 2022, and references herein]. The opening of the Drake Passage at 33 Ma (Figure 6), in response to seafloor spreading along the Scotia Ridge [Lagabrielle et al., 2009, and references herein], crosscut the Southern Andean Cordillera leading to two separated strongly attenuated remnant cordilleras. The volume and elevation of the former continuous cordillera remain unknown, but comparison with some portions of the current Andes north of the Chile Triple Junction can be proposed (Figure 5A–B).

4. A theoretical model of "active continental margin orogenic cycle"

The evolution of the Antarctica–South America connection leads us to highlight a causal link between the sites of opening of slab windows and the attenuation and disappearance of a former continuous cordillera. Situations involving more than one ridge subduction in one single region are rare on Earth, but

they cannot be neglected. We will comment in Section 5 the case Sundaland that has been concerned by the subduction of two ridges leading to widespread extension in the upper plate. Most of the situations however involve the subduction of one ridge. Here we attempt to design a theoretical evolution for active continental margin with cordillera which focuses on the variations of slab forces before, during and after the subduction of a single spreading ridge segment (Figure 7). We assume that the ridge intersects the trench at a low angle.

The evolution can be divided into three stages. During stage 1 (cartoons 1 and 2, Figure 7), the ridge remains far from the trench and the age of the ocean lithosphere decreases oceanward from the trench. We assume that slab pull is efficient as a large amount of relatively old lithosphere is descending in the subduction zone. Therefore, coupling at the subduction interface is supposed to remain high during stage 1 and a compressional regime develops in the continental plate triggering the construction of an elevated cordillera. Analogue models have shown that an increase of shortening is observed in the overriding plate during the subduction of increasingly young oceanic lithosphere in the case the overriding plate moves toward the trench faster than slab retreat [Salze et al., 2018].

During stage 2, the ridge enters the trench (cartoon 3, Figure 7). Now, the oceanic lithosphere gets older seaward. Interplate coupling decreases due to rapid thermal weakening at the plate interface; in a same sense, slab pull force is greatly reduced because a slab window opens beneath the forearc domain.

During stage 3, the oceanic lithosphere is older oceanward (cartoons 4 and 5, Figure 7). The slab-window continues to develop and migrates beneath the upper plate. A high thermal regime occurs beneath the continental lithosphere and the overriding plate records long-wavelength thermal doming as suggested by field studies in the Patagonian Cordillera (cartoon 4, Figure 7) [Scalabrino et al., 2010, 2011]. In cartoon 5, the slab-window is largely opened and a thermal erosion occurs at the base of the continental lithosphere. The tectonic regime of the cordillera is now dominated by local to regional extension with negative inversion of the main thrusts.

After a few millions of years, the slab window opens largely and the asthenospheric mantle is able
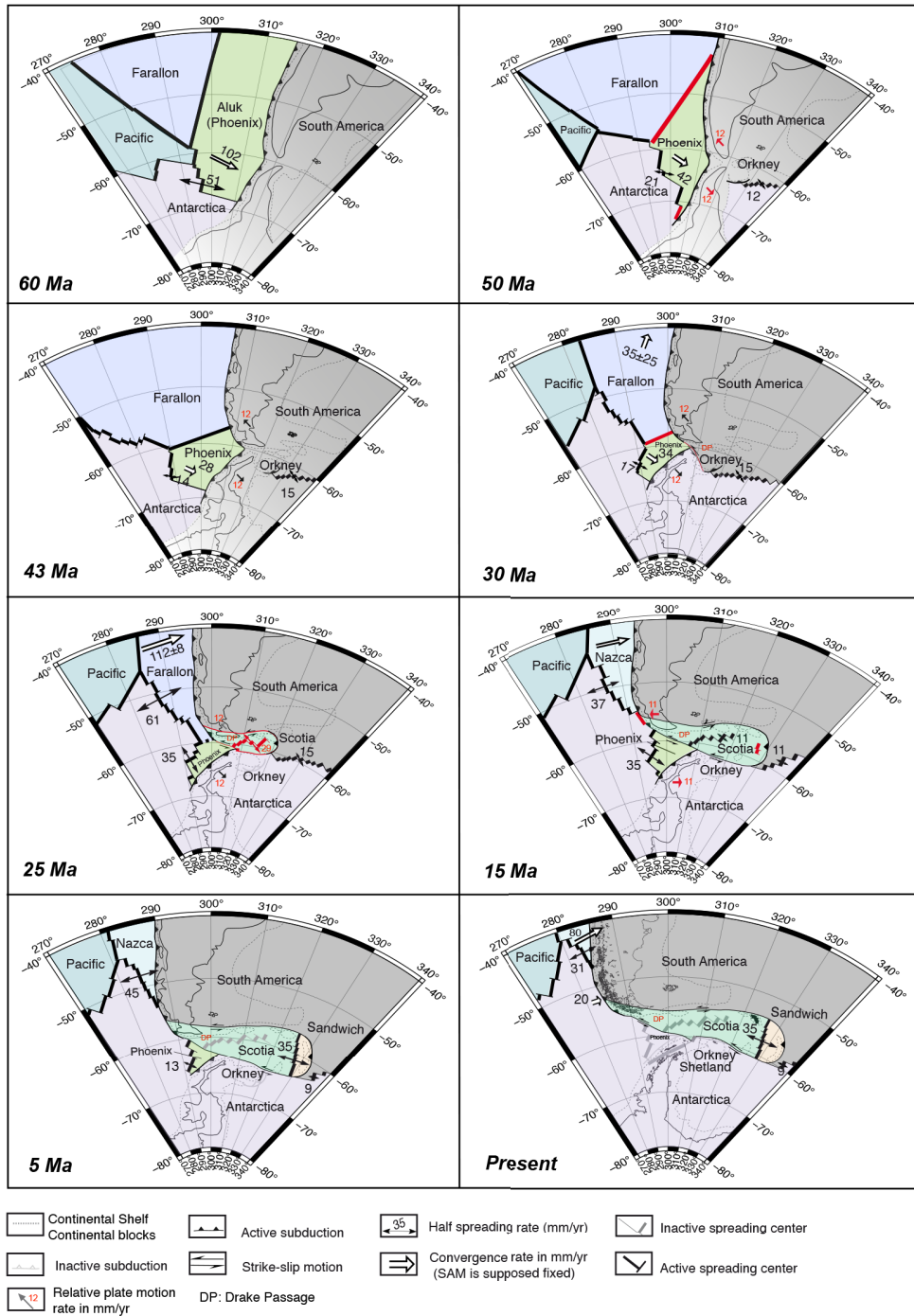
Figure 6. Schematic kinematic reconstructions of South America–Antarctica since 60 Ma, showing relations between active spreading ridges subductions and Scotia Sea back arc expansion. General stereographic projection (using GMT software), after Scalabrino et al. [2009].
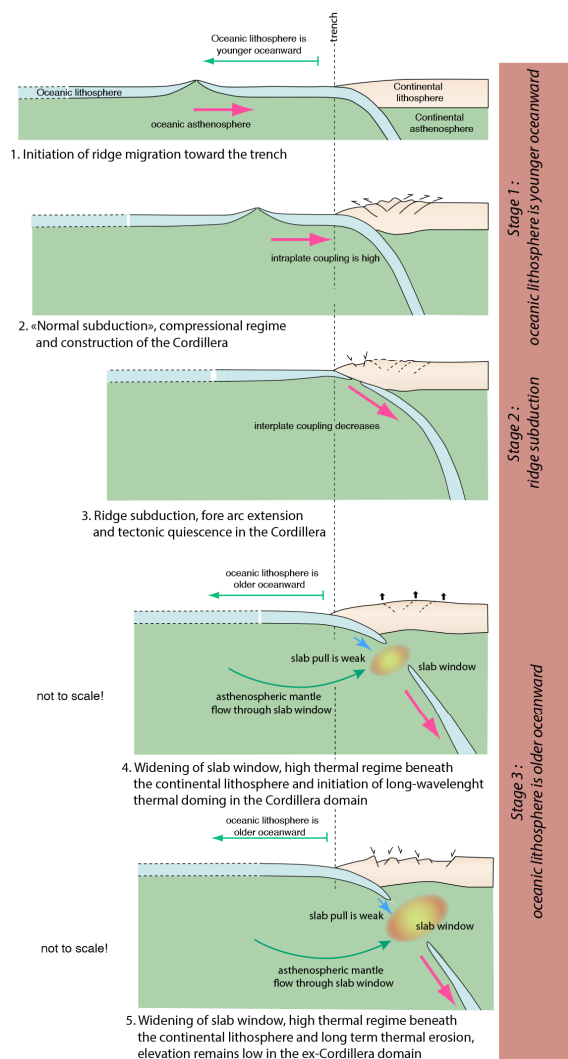
Figure 7. Multi-stage theoretical model of continental margin evolution during and after active spreading ridge subduction and slab window formation (see comments in text).

to flow from the oceanic domain through the window to maintain a large thermal anomaly beneath the upper plate, favoring thermal erosion. In addition, slab pull is reduced to almost zero and the coupling at the interface might still be low. These parameters maintain low tectonic coupling at the subduction interface.

Numerical models designed to investigate the effects of the complete subduction of an oceanic plate suggest that the arrival of a mid-ocean ridge at the trench is preceded by a slab detachment due to

a reduction in strength and negative buoyancy of the approaching oceanic lithosphere and the loss of transmission of the slab pull force to the surface [Burkett and Billen, 2009, Wu et al., 2022b]. In terms of mantle dynamics, a complex mantle circulation begins beneath the upper plate. Laboratory models of mantle dynamics through slab gaps highlight that lateral, poloidal and toroidal flow patterns affect a large part of the subduction zone which may result on some variations of the spatio-temporal behavior of the overriding plate [see Guillaume et al., 2010, Király et al., 2018, 2020].

A remarkable feature displayed by large peri-Pacific subduction boundaries is their geographical stability over hundred millions of years. This is well demonstrated for the successive Ecuador–Peru–Chile arcs that moved only some dozen of kilometers apart from an average position on the western side of South America [e.g. Ancellin et al., 2017]. For this reason, during their long evolution, the Andean-type cordilleras are able to record all types of margin morphologies and structure [Allmendinger et al., 1997, Armijo et al., 2015, Oncken et al., 2006, Ramos, 2009, 2014, Russo and Silver, 1996]. Indeed, during its Mesozoic–Cenozoic evolution, the Andes region changed from a very low elevation area dominated by marine sedimentation to a 400 km wide uprising continental plateau, that reached an elevation of 3500–4000 m during a relative short period of about 20 Ma (see Figure 5A–B) [e.g. Armijo et al., 2015]. Inversely, we recalled above that around 33 Ma, southernmost South America underwent progressive subsidence and completely disappeared below sea-level in relation to the opening and widening of the Drake Passage (Figure 5B). This implies that at the geological scale, the reliefs of subduction cordilleras are not stable features, they may change from elevations close to sea level to very elevated plateaus that in turn may resume to sea level elevations. We thus evidence an "active continental margin orogenic cycle" including birth, growth, attenuation and disappearance of subduction cordilleras. Part of this cycle is controlled by the subduction of active spreading ridges.

5. Discussion: what about the rest of the world?

In the following, we will explore how geological constraints around the world allow to confirm that subduction of active spreading ridges triggers significant

changes in the behavior of the upper plate continental lithosphere, inducing notably subsidence and attenuation of former cordilleras.

5.1. *North East-Pacific: from Aleutian-Alaska to Central America*

The North-Eastern Pacific margin is integrated into a long-lived history of oceanic subductions beneath continental lithosphere involving oceanic plates or micro-plates since the Mesozoic. Most of these continental active margins exhibit high-elevation cordilleras in response to magmatic and tectonic crustal thickening. Through time, compressional shortening was not the unique factor of tectonic evolution of the North-Eastern cordilleras as evidenced by several phases of extensional deformation related to the complex and long-term subduction of spreading ridges. In this section, we describe how active spreading ridge subductions during the Cenozoic induced particular changes in the tectono-magmatic evolution of cordilleras from Aleutian-Alaska to the Central America region.

5.1.1. *Subduction of active spreading ridges along the North-Eastern Pacific since the Cenozoic*

During the Cenozoic, the northwestern margin of North American plate (including the East Aleutian arc, Alaska, British Columbia and Oregon) was the site of multiple active spreading ridge subductions [Breitsprecher et al., 2003, Fuston and Wu, 2020, Madsen et al., 2006, Müller et al., 2008, 2016, Sisson et al., 2003, Sisson and Pavlis, 1993, Thorkelson et al., 2011]. Cenozoic plate kinematic reconstructions highlight three subductions of oceanic plates/microplates located northward of the Pacific plate, namely the Resurrection, the Kula and the Farallon plates (Figure 8) [e.g. Fuston and Wu, 2020, Madsen et al., 2006]. These plates were separated by four spreading axes: the Kula/Resurrection Ridge (KRR); the Resurrection/Farallon Ridge (RFR), the Kula/Farallon Ridge (KFR) and the Pacific/Farallon Ridge (PFR); all of them were progressively subducted beneath the North American plate (Figure 8).

5.1.2. *Aleutian-Alaska*

The Alaska active continental margin offers a clear example of the transition between an elevated subduction cordillera, the Alaska belt, to a low elevation belt, finally passing to a succession of volcanic islands forming the Aleutian arc [Jicha et al., 2004]. The significance of such a rapid transition between a high elevation cordillera to an island arc is not yet explored and no evidence of dramatic crustal extension was reported at the Alaska western border, in the transition to the Bering sea. Due to the geometry of the NW–SE KRR with respect to the arcuate active margin, the KRR/North America triple junctions followed two different configurations (Figure 8): a high-angle intersection from the Aleutian to the Sanak-Baranof (Alaska) margins from 80–55 Ma and a low-angle intersection along the northern British Columbia between 50–35 Ma [Breitsprecher et al., 2003, Cole and Stewart, 2009, Farris and Paterson, 2009, Fuston and Wu, 2020, Kusky et al., 1997, Madsen et al., 2006, Sisson et al., 2003].

Together with the CTJ region, the eastern Aleutian arc has long been a reference for studies of slab window effects. It has been shown that slab window opening has a profound influence on continental margin magmatism with the formation of mantle-derived magmas intruding accretionary wedges. The upwelling of suboceanic mantle beneath a continental margin triggers the generation of magmas by partial melting of overlying crustal rocks and/or by decompression melting of the upwelling mantle [Cole and Stewart, 2009, Cole et al., 2006, D'Orazio et al., 2001, Sisson et al., 2003, Sisson and Pavlis, 1993].

When considering the tectonic evolution of cordilleras, it is important to point that the Aleutian arc region and southern Alaska slab window volcanism was coincident with HT-LP metamorphism and crustal extension [Bradley et al., 2003, Groome et al., 2003, Iwamori, 2000, Sisson et al., 1989, Underwood et al., 1999]. Zones of local extension developed within arc-front, forearc, and accretionary prism settings. For example, the late Paleocene to Eocene Caribou Creek volcanic field (Southern Alaska) was erupted in a zone of extension that trended orthogonally to the continental margin (Figure 8) [Bradley et al., 2003, Cole and Stewart, 2009]. Infra-arc tectonic extension caused long-arc differences in the nature of crystallization, facilitated by changes in the thermal and density structure of the subarc lithosphere [Singer and Myers, 1990, Singer et al., 1992]. Cole and Stewart [2009] note that in order for basalts or gabbros to retain their mantle signature, the mafic

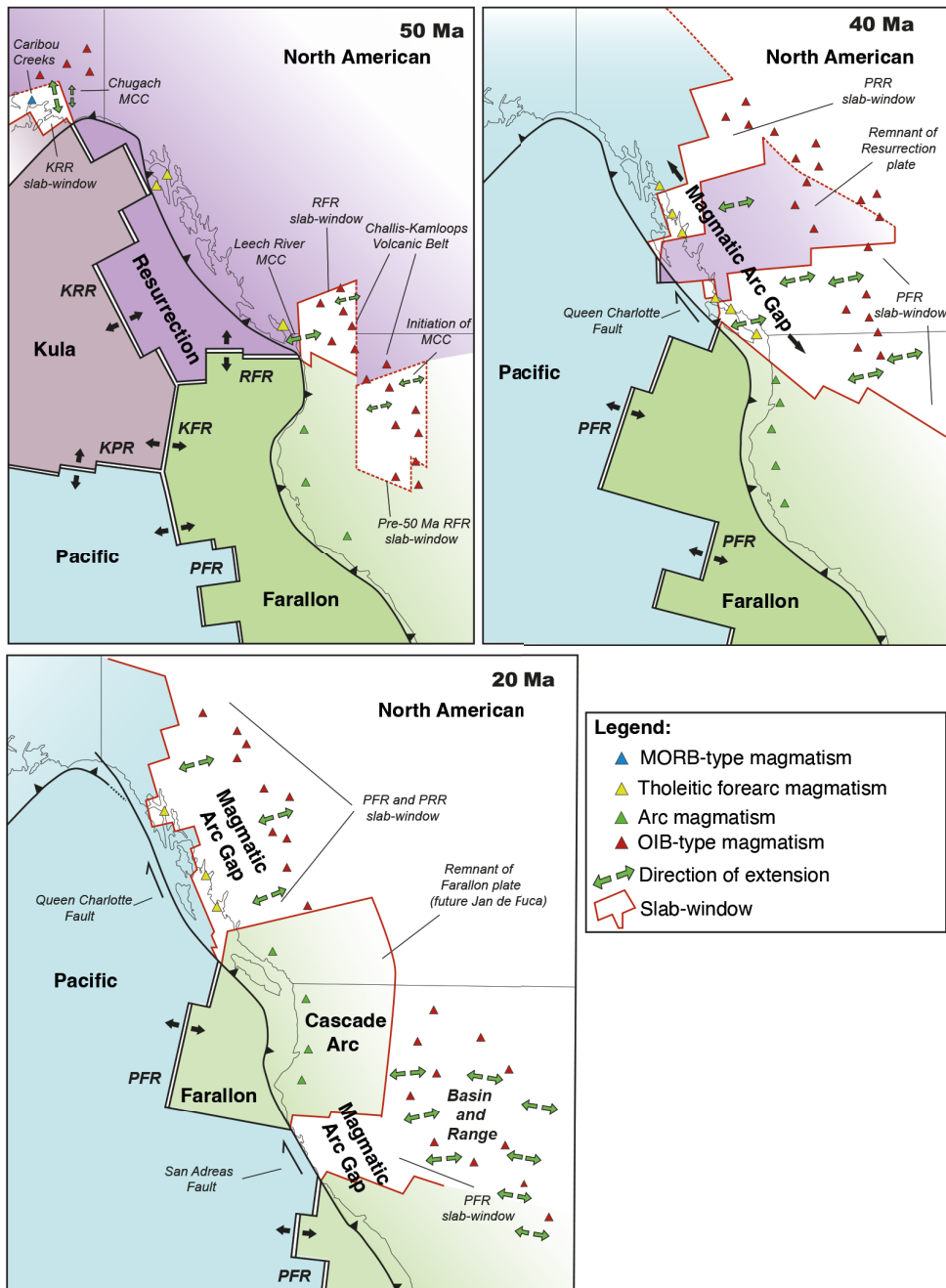**Figure 8.** Cenozoic plate configuration around the northwestern American margin and synthesis of tectono-magmatic events at 70 Ma, 50 Ma and 30 Ma. Positions of active spreading ridges and slab windows come from Madsen et al. [2006] and Fuston and Wu [2020]. KRR: Kula/Resurrection Ridge; KPR: Kula/Pacific Ridge; RFR: Resurrection/Farallon Ridge; KPR: Kula/Pacific Ridge; PFR: Pacific/Farallon Ridge.

magmas need pathways to reach shallow crustal levels. These pathways are more easily formed during crustal extension. Crustal extension was also described in the Alaskan back-arc domain coeval to alkaline magmatism right above the slab-window (Figure 8) [Bradley et al., 2003]. Locally, HT-LP metamorphism was associated with Metamorphic Core Complex exhumation as shown around the central margin of Alaska [53–50 Ma Chugach MCC, Pavlis and Sisson, 1995, Sisson and Pavlis, 1993].

5.1.3. *Northern American Cordillera*

After a Mesozoic–Early Cenozoic complex evolution of terrane accretions along the Northern America Cordillera [see Clennett et al., 2020, for a synthesis], the entire Northern American active margin has been subjected to spreading axis subductions. Synchronously to the eastward subduction of the KRR along the Alaskan margin, the RFR entered the subduction along the Northern American Cordillera (Figure 8) [e.g. Fuston and Wu, 2020]. The related triple junction migrated northward close to the Vancouver Island [Madsen et al., 2006, Fuston and Wu, 2020]. Since Late Eocene–Oligocene times, multiple slab-windows related to KRR, RFR and KFR subductions have developed inducing a composite large-scale pathway for asthenospheric flows still observable beneath British Columbia (Figure 8) [Breitsprecher et al., 2003, Severinghaus and Atwater, 1990, Madsen et al., 2006, Thorkelson et al., 2011]. A composite slab-window is also responsible of the break-off of the Resurrection slab [the "Yukon" slab according to Fuston and Wu, 2020] forcing the dynamics of the British Columbia margin to switch from a convergent to a transcurrent lithospheric boundary at 40 Ma (the Queen Charlotte dextral fault system). Today, the Juan de Fuca oceanic plate (a remnant of the Farallon plate) intersects the continental margin with two related triple junctions, the Explorer Triple junction close to Vancouver Island and the Mendocino triple junction north of the Californian state.

Before slab-window interactions, the North American Cordillera was the site of a complex magmatism evolution inducing two main igneous domains from west to east and separated by a North–South Sr–Nd isotopic limit: the western Cordillera mainly dominated by mantle magmas and the eastern Cordillera with crustal magma affinities [Kistler and Peterman,

1973, Leeman et al., 1992]. The Cenozoic-Quaternary influence of hot asthenospheric flow through slab-window and/or gaps is well evidenced by studies of magmatic products from the forearc and back-arc domains. During Eocene–Oligocene times, the voluminous forearc magmatism of the Canadian Cordillera bears tholeiitic and alkalic signatures and was emplaced in an extensional/transtensional setting (Figure 8) [Barnes and Barnes, 1992, Davis et al., 1995, Hamilton and Dostal, 2001, Thorkelson et al., 2011]. More inland, the Cenozoic Canadian magmatism varies from north to south. Intraplate magmatism signature is localized along a major part of the British Columbia Cordillera, whereas the Cascadian Arc exhibits a typical calc-alkaline character (Figure 8) [Thorkelson et al., 2011]. A key feature of the Cenozoic magmatic evolution occurred at ca. 47 Ma with the cessation of arc-like magmatism switching to an intraplate activity from Late Oligocene to Holocene [Edwards and Russell, 2000, Madsen et al., 2006, Thorkelson et al., 2011]. This transition occurred during the development of the Northern Cordillera slab-window, below a 1500 km-long transect from south British Columbia to the northwestern tip of Canada. Along this last region, adakitic magmatism was emplaced just above the slab-window edge (Figure 8) [e.g. Thorkelson et al., 2011]. The Northern American Cordillera is also characterized by a change in the deformation regime. Until early Cenozoic times, a compressional regime was responsible for crustal thickening, metamorphic core complex (MCC) initiation and Andean Altiplano-like cordillera [Coney and Harms, 1984]. This stage is followed in Cenozoic times (starting in the Eocene) by tectonic extension inducing thinning of the crust and denudation of MCC [Coney and Harms, 1984]. The present architecture of the British Columbia and Washington region derives mainly from this Eocene extensional event [Parrish et al., 1988]. For Edwards and Russell [1999], the Northern Cordilleran Volcanic Province can be considered as a northern Basin and Range model where MCC are associated with HT-BP metamorphism (Figure 8). This is the case for the Early-Middle Eocene complexes of the Leech River (south of Vancouver Island) [Groome et al., 2003] and the Challis–Kamloops (south of British Columbia and northwest of United States) where magmatism occurred during the formation of a pull-apart basin and MCC exhumation [Breitsprecher et al., 2003, Parrish

et al., 1988]. Finally, high heat flow and thin litho-sphere of the northern Cordillera [60–52 km, Harder and Russell, 2006] demonstrate the impact of the thermal erosion of the lithospheric mantle linked to hot mantle upwelling.

5.1.4. *California and Basin and Range*

South of the Northern Cordillera, the California margin was also deeply affected by active spread-ing ridge interaction. During the Oligocene, the PFR entered the subduction (Figure 8) and a PFR-related transform fault collision (probably) led to the initiation of the transcurrent dextral fault system of San Andreas [Atwater, 1970, Dickinson and Sny-der, 1979, Severinghaus and Atwater, 1990]. From 30 to 15 Ma the progressive opening of a slab win-dow led to subsequent active mantle upwelling be-neath the western United States. Two triple junc-tions, the Mendocino and Rivera triple junctions, then migrated in opposite directions along the con-tinental margin in relation with the growth of the San Andreas transform fault. The slab window continued to widen as both triple junctions propagated north and south. This process explains the shutdown of the previous magmatic arc as the San Andreas Fault developed.

Fernandes et al. [2019] realized a synthesis of Cenozoic topographic evolution of Northwestern and Western America coupling stratigraphic and ge-omorphic markers. They highlight a series of uplift pulses characterized by a total of more than 2 km high long-wavelength surface uplift. Correlations between thermochronology, magmatism and syn-tectonic sedimentation analysis also suggest that a Late Mesozoic regional compressive regime evolved toward a regional extensional regime also described northward by Coney and Harms [1984] [see Fer-nandes et al., 2019, for references]. This overall ex-tensional deformation is well documented in the Basin and Range Province where Late Oligocene?–Miocene MCC formed (Figure 8). These features accommodate considerable amounts of horizontal displacements in the middle crust along low-angle normal faults. In the upper crust, normal faulting with high angle faults control the formation of nu-merous grabens and subsiding basins infilled by syn-extensional sediments [Faulds et al., 1990, Faulds and Varga, 1998, Malavieille, 1987, Varga et al., 1996, Wer-nicke, 1981, 1985, Wernicke et al., 1987, Wernicke,

2009]. This area was also subjected to mid-Miocene intensive intraplate eruption from the Colorado River Plateau [Dickinson, 1997, 2006, Roberts et al., 2012, for references] to the south of California [Cole and Basu, 1992, Wilson et al., 2005].

Dickinson [1997] and Dickinson and Snyder [1979] first pointed to the correlation between extensional tectonics in the Basin and Range Province and the opening of the slab window beneath western North America. They suggest that upwelling asthenosphere heated the base of the lithosphere and caused its weakening. The hypothesis of a hot mantle anomaly is enhanced by the regional-scale uplift that does not involve crustal thickening [Lewandowski et al., 2018].

Therefore, the dynamic topography observed in California and surrounding areas reflects long-term thermal anomalies driven by asthenospheric upwelling through slab-windows or related-slab-window gaps. These deep processes have induced the thinning of the lithosphere [ca. 70 km; Klölcling et al., 2018] via thermal erosion of the lithospheric mantle and extensional deformation of the upper plate since middle Cenozoic. We must note that in the Basin and Range region, the extensional tecton-ics applied to a former collisional orogen having a thickened crust. This allowed the continental crust to return to a former thickness of 30 km by extensional collapse [Dewey, 1988, Coney and Harms, 1984].

Comparisons between the northern and south-ern cordilleras of North America finally confirm that the context of active ridge subduction impacts a large panel of characteristics of the overriding plate. Switches from convergent to transcurrent boundary conditions (transcurrent strike-slip systems of Queen Charlotte and San Andreas Faults) associated with hot asthenosphere flowing through slab window fa-vor extension of cold lithosphere. In this context, the variability of extension styles affecting the cordilleras is controlled by the rheological and thermal state of the overriding crust [Buck, 1991, Rey et al., 2001].

5.1.5. *Baja California*

The Baja California and western regions of Mex-ico mainlands (from Sonora to Jalisco) belong to the southern part of Laramide orogen. During Cretaceous to Eocene times, they experienced a magmatic-tectonic evolution in relation to the sub-duction of the Farallon plate beneath the northern
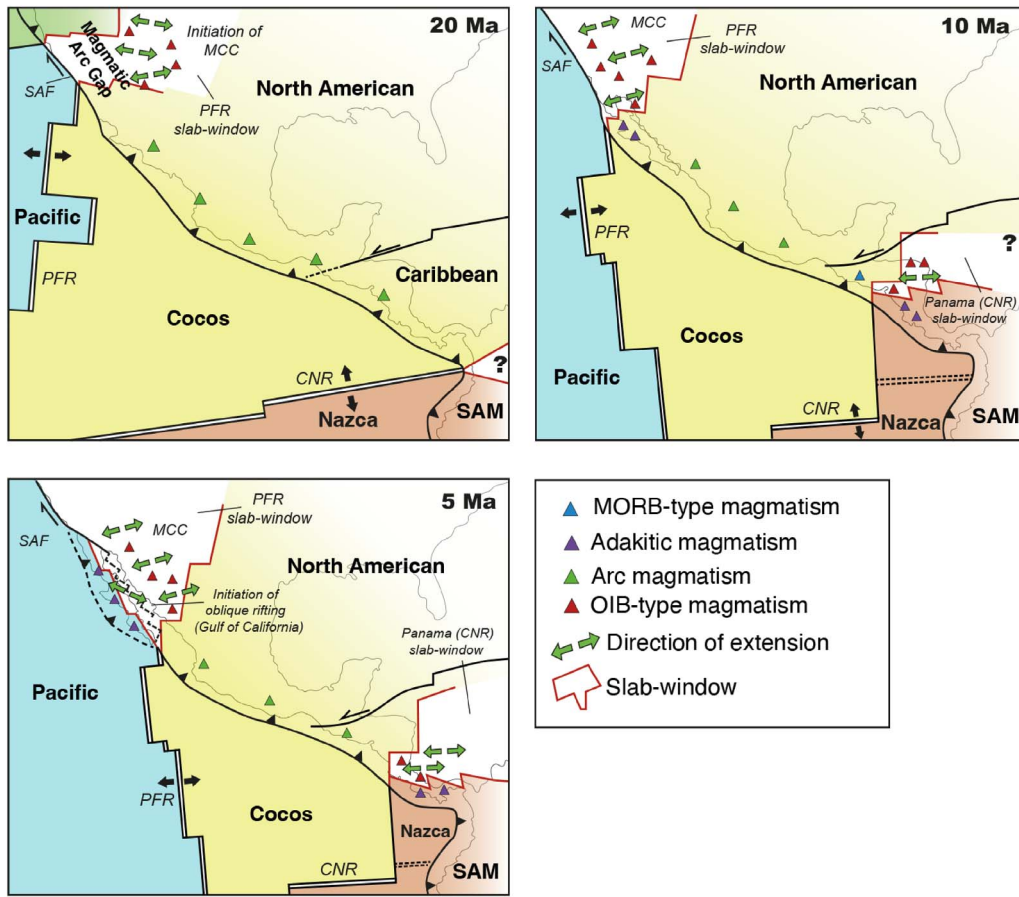
Figure 9. Cenozoic plate configuration around the Central American margin and synthesis of tectono-magmatic events at 20 Ma, 10 Ma and 5 Ma. Position of the active spreading ridges from 20 Ma and 5 Ma come from Bourgois and Michaud [2002], Johnston and Thorkelson [1997], Morell [2015]. PFR: Pacific/Farallon Ridge; CNR: Cocos/Nazca Ridge; SAF: San Andreas Fault; SAM: South American Plate.

America plate, involving variability of subduction rates and slab dips [Coney and Reynolds, 1977, Engebretson et al., 1985, Ferrari et al., 2006, Keith, 1978]. Progressive eastward subduction of oceanic plates was also responsible for the middle Miocene to Present recycling of the East Pacific Ridge (EPR) beneath Baja California and Mexico, where the Mexico triple junction has migrated to the south with trench-parallel slab window opening (Figure 9) [Bourgois and Michaud, 2002, Michaud et al., 2006]. During the early Pliocene, the fragmentation of the Pacific plate leading to the creation of the Rivera plate, induced a jump of the triple junction, which is now located southeastward [Bourgois and Michaud,

2002, Michaud et al., 2006]. Contemporaneously to the Basin and Range Province, Baja California and the western Mexican region were affected by Late Oligocene–Late Miocene continental-scale extension responsible of OIB-type magmatism in the upper plate and of the initiation of Metamorphic Core Complex exhumation (Figure 9) [see Calmus et al., 2015, for references]. The overall regions experienced a major alkaline magmatic event, dated from 11 Ma to present, with volcanics emplaced along an E–W trending corridor from Jalisco to Mexico City [Ferrari et al., 2006]. To the northwest, the Gulf of California corresponds to a 1300 km-long corridor extending from the southern tip of the San Andreas Fault

to the Mexico triple junction to the south. On the western flank of the Gulf of California, the presence of bajaites with adakitic magmatic affinities, suggests subduction of a very young oceanic lithosphere (Figure 9) [Aguillón-Robles et al., 2001]. Based on these results, Bourgois and Michaud [2002] propose that the slab window development beneath southern Baja California and mainland Mexico (30° to 18° N) resulted from the subduction of the East Pacific rise.

Oblique rifting in the Gulf of California and extensional deformation in the surrounding regions of Mexico were accentuated from 12 Ma to 6 Ma (Figure 9) [Stewart and Roldán-Quintana, 1994, Stock and Hodges, 1989]. Crustal extension is correlated with a regional scale uplift [e.g. Calmus et al., 2015, Ferrari et al., 2013, Mark et al., 2017] with a notable increase of uplift rates (0.1 to 0.2 mm/yr) starting at 15 Ma [see Stephenson et al., 2014, for a synthesis]. Recent extension, local uplift and alkaline magmatism are associated with high surface heat flow from 83 mW/m^2 to 90 ± 27 mW/m^2 [Ziagos et al., 1985, Pérez-Campos et al., 2008], suggesting a mantle origin for these surface processes. As indicated by Bourgois and Michaud [2002], oblique rifting and oceanic seafloor spreading in the Gulf of California occur right above the slab window related to the subduction of the EPR (Figure 9). During its southeastward migration, this window allowed upwelling of asthenospheric flows inducing progressive weakening of the continental lithosphere and subsequent increase of extension and magmatism in the upper plate.

5.1.6. *Central America*

Central America, and more specifically Costa Rica and Panama, are the site of the interaction of multiple plates including the North American, South American, Cocos, Nazca and Caribbean plates. The Cocos–Nazca spreading system initiated at around 25 Ma [Hell, 1977] and progressively subducted beneath the Central America (Figure 9). Thus, between 10 Ma and 2 Ma, Central America was swept by a restricted slab window, the Panama slab-window, related to the buried Cocos–Nazca spreading axis (CNR, Figure 9) [Johnston and Thorkelson, 1997, Thorkelson et al., 2011]. At present, the corresponding triple junction corresponds to a trench–trench–transform configuration where the subduction of the Panama Fracture Zone forced

the northeastward movement of the slab-window [Johnston and Thorkelson, 1997]. Magmatic interactions of the Panama slab window on the Costa Rica/Panama areas and on the Caribbean plate are well-documented. Here, late Miocene to Pleistocene dacites and rhyolites rocks with adakitic signatures located in the forearc of Panama and southern Costa Rica correspond to the trailing edges of the slab-window (Figure 9) [Johnston and Thorkelson, 1997]. OIB-type magmatic activity is also observed onland, on the Caribbean plate whereas Nicaragua, El Salvador and Guatemala lavas display arc compositions (Figure 9). Therefore, the Panama slab window corresponds to a pathway for voluminous flows of enriched sub-slab peridotite into the arc and back-arc domains [Johnston and Thorkelson, 1997]. Based on geochemistry analysis of hydrothermal fluids, Bekaert et al. [2021] confirm that the Panama window allows eastward intensive asthenospheric flows coming from the Galapagos hot spot. This observation correlates with seismic anisotropy data showing W–E trending flows beneath the Caribbean plate [Russo and Silver, 1994]. Tectonically, the evolution of the region results from several phases of deformation related to: (1) the subduction of the Cocos plate, (2) the subduction of the ridge-transform system of Nazca–Cocos, (3) the opening of the Caribbean basin and, (4) the subduction of the aseismic Cocos ridge.

In central America, an epeirogenic uplift event occurred between 10 and 6 Ma with north-striking late Miocene–Holocene grabens (Figure 9) disrupting a middle-Miocene ignimbrite layer [Rogers et al., 2002]. These authors attribute this event to an upwelling of mantle asthenosphere through a tear linked to the slab detachment during the Cocos ridge collision. Nevertheless, the uplift and the trench-orthogonal extensional deformation are synchronous with the slab-window development beneath the southern Central America (Figure 9). In such a configuration, voluminous mantle flows from the Galapagos hot-spot may have disrupted the thermal state of the upper plate further north and east from the predicted slab-window position. Finally, this region is governed by complex interactions of subduction processes, involving normal subduction, recycling both spreading and aseismic ridge in a short time. In consequence, the 4D evolution of the mantle dynamic beneath Central America and its impacts on the upper plate remain difficult to fully assess.

5.2. *West-Pacific: from the Philippine Sea plate to the Kuril arc*

The West Pacific active margins include subduction of oceanic lithosphere beneath both continental and oceanic lithosphere. The continental active margins forming the easternmost edge of the Eurasia plate are characterized by relatively low elevation regions and the lack of prominent active compressional cordilleras (Kamchatka, Kuril, Japan). By contrast to the margins of North and South America, the Western Pacific continental margins exhibit a number of back-arc basins resulting from the extension of the continental crust and/or intra-arc tearing, and subsequent localized accretion of oceanic crust. These basins show complex histories, but opened generally in a short time span, between 30 to 10 Ma [Park et al., 1990]. In this section, we first describe the subduction of the Izanagi–Pacific Ridge (IPR) beneath the Eurasian margin during Cenozoic times. We further focus our discussion on some local and regional geological consequences of the IPR subduction and its migration through the Philippine-Borneo region, the South China Sea, Japan and Kuril regions.

5.2.1. *Subduction of the Izanagi–Pacific Ridge and Wharton Ridge along the Eurasian margin*

During Mesozoic to Cenozoic times, the Eurasian margin along East Asia was affected by extensive subduction along an up to 6000 km long active margin [Müller et al., 2016, Torsvik et al., 2019] including several related processes including trench retreat, slab roll-back and subduction of active spreading ridges. Process of spreading ridge subduction has been described for several decades especially in the regions surrounding Japan coastlines. Here, two opposites reconstructions of interaction between the Asian margin and active spreading ridge have been proposed involving the Izanagi–Pacific Ridge (IPR). The first one, suggested by Maruyama et al. [1997], corresponds to a frontal ridge–trench interaction where the IPR intersects the Asian continental margin at a high angle. The related trench–trench–ridge triple junction migrated from south to north from Late Cretaceous to Eocene times. The second one, based on large-scale reconstructions of the Pacific hemisphere starting at 140 Ma [Müller et al., 2008], hypotheses

that the western part of the Pacific floor was created by a NNE–SSW, 3000 km-long spreading ridge that kept remarkably parallel to the active margin of Eurasia between 110 and 70 Ma. In this reconstruction (Figure 10), a low-angle ridge–trench interaction was proposed where the IPR entered the subduction zone in one piece between 60 and 50 Ma [Whittaker et al., 2007, Seton et al., 2015, Wu and Wu, 2019]. This implies that the entire border of the Eurasian plate was concerned by the opening of a mega-slab window continuously widening beneath the continent as subduction continued. In addition, high-resolution tomography records of East Asian mantle as well as numerical modelling of mantle structure and dynamics provide spectacular images of a large slab-window opened between the Izanagi and Pacific plates following the early Cenozoic subduction of the active IPR [Wu et al., 2022a]. Recent kinematic models confirm the low-angle Izanagi–Pacific ridge–trench interaction with Eurasia at 50 ± 10 Ma but limit the ridge subduction between Korea, Japan and the Russian Far East [Wu et al., 2022a] instead of Müller et al. [2008] models that involve the entire East Asian margin from Borneo to Kuril areas (Figure 10). An active spreading subduction process is also noted along the southwestern tip of the East Asian margin. From Late Cretaceous to Early Eocene periods, the northeastward subduction of the Wharton Ridge (WR), an active spreading ridge between Indian and Australian plates (Figure 10), led to the development of a slab window beneath the Sundaland [Whittaker et al., 2007]. The entire region was concerned by two opposite-vergent subductions of spreading axis: the IPR with a southwest vergence and the Wharton ridge with a northeast vergence (Figure 10).

5.2.2. *The Philippine and Borneo area*

The Philippine and Borneo Region (PBR) was affected by a long-lived subduction process since Mesozoic times causing complex and spectacular opening of back-arc extensional basins together with various magmatic signatures on the upper plate [see Burton-Johnson and Cullen, 2022, for references]. The rifting history of South China Sea region, including Philippine and Borneo, shows the initiation of extensional deformation lasting from 62 Ma to 45 Ma [Cullen, 2010, Zhang et al., 2020]. This
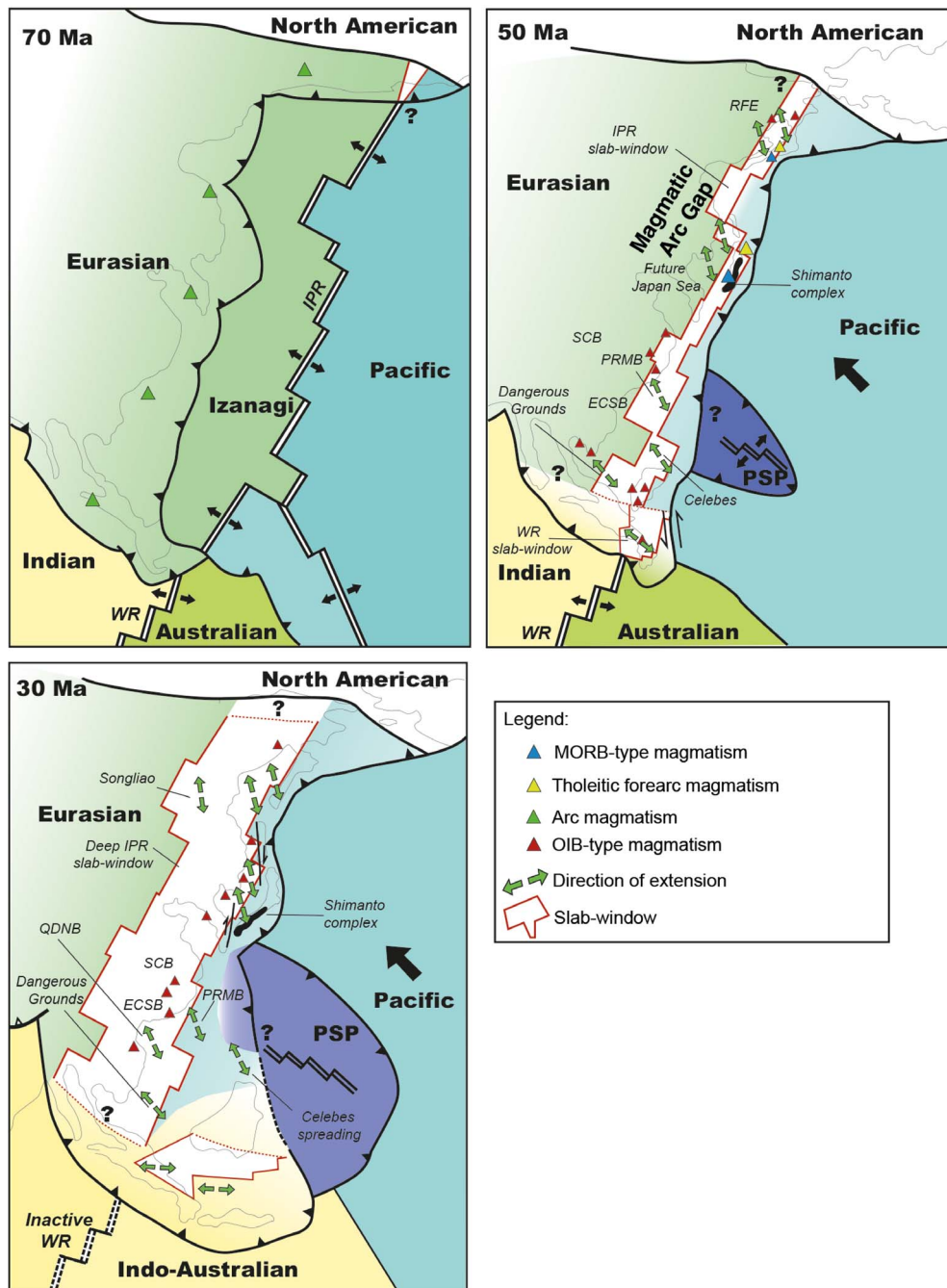
Figure 10. Cenozoic plate configuration around the Southeast Asian margin and synthesis of tectono-magmatic events at 70 Ma, 50 Ma and 30 Ma. Position of active spreading ridges at 70 Ma come from Müller et al. [2008], Whittaker et al. [2007]. IPR: Izanagi/Pacific Ridge; WR: Wharton Ridge; RFE: PSP: Philippine Sea Plate; Russian Far East; SCB: South China Block; ECSB: East China South Block; PRMB: Pearl River Mouth Basin; QDNB: Qiongdongnan basin.

event is well documented in the Dangerous Grounds, where Paleocene to Middle-Eocene extensional deformation causes continental rifting between Vietnam, Indonesia and Borneo Islands (Figure 10) [e.g. Burton-Johnson and Cullen, 2022]. To the east, rifting started from 50 to 40 Ma and was responsible for the extension in the Celebes and Sulu basins (Figure 10), followed by initiation of oceanic spreading at 45 Ma and 35 Ma respectively [e.g. Burton-Johnson and Cullen, 2022]. The early Cenozoic intraplate rifting event in this region is well documented by: (1) regional geology, (2) geochemical evolution characterized by low volumes of OIB magmas, and (3) geophysical data. Burton-Johnson and Cullen [2022] suggest that slab retreat is a dominant process able to trigger extension in the Celebes and Sulu basins and exclude extrusion, mantle plume or slab pull of the Proto-South China Sea subduction. Their model of extension during the Cenozoic period also shows that an active spreading ridge center interacted with the eastern margin of SE Asia during the Eocene but do not discuss its impact on the evolution of the overriding plate. Kinematic reconstructions by Müller et al. [2008] show that the PBR was affected by the Early Cenozoic subduction of the NE–SW IPR. In this configuration, the IPR interacted with the SE Asian margin southeast of Borneo and migrated northeastward inducing the progressive opening of a large slab-window beneath the PBR (Figure 10). Together with IPR recycling, the Wharton Ridge subducted leading up to the opening of a slab window beneath the southern tip of Borneo region (Figure 10). Rising of hot material during this time induced dynamic uplift with basaltic magmatism in Borneo and Indochina and surrounding extensional basins since the Early Cenozoic [Fyhn et al., 2009, Roberts et al., 2018, Yan, Q. et al., 2018]. It is important to point that in such reconstructions, the entire region was the site of a complex subduction process involving a double opposite-vergent subduction of active spreading ridges (IPR to the east and Wharton to the west) from 65 to 45 Ma (Figure 10). This situation was responsible for the opening of a double opposite slab-window allowing upwelling of a large amount of hot asthenospheric mantle, triggering in turn the initiation of lithospheric extension in the upper plate, coupled with intraplate OIB-type magmatism during late Cretaceous to Early Cenozoic times.

5.2.3. *South East China*

During Permian to Early Cretaceous times, South East China was marked by the development of subduction-type orogens, locally thickened by accretion of mantle-derived magmas. Emplacement of large amounts of Mesozoic granitoids in South East China was accompanied by thermal softening and gravitational instability allowing extension of the crust [Faure et al., 2016]. Therefore, during Middle Jurassic to Late Cretaceous times, the Pacific coastal region of China was characterized by Basin and Range type province, notably in the South China block (SCB). But this widespread Mesozoic extensional event cannot be related to any documented slab window development beneath the region [Faure et al., 2016, Wang and Shu, 2012].

During the Late Cretaceous-Cenozoic, the tectonic evolution of the South China domain was controlled by successive stages of subduction of the Pacific lithosphere including the subduction of the IPR beneath the Eurasia active margin (Figure 10) [e.g. Brown et al., 2022, Wang et al., 2022]. A recent analysis of present residual topography indicates an abnormal hot mantle beneath the entire East Asian margin [Hoggard et al., 2017, 2021]. This hot anomaly has produced local to regional dynamic uplift and subsidence, evidenced by a series of geological records as follows. (1) To the south, the northern margin of the South China Sea experienced uplift events since the Eocene coupled with syn-rift tectonic subsidence [e.g. Brown et al., 2022]. This is the case for the Pearl River Mouth Basin (PRMB) where Suo et al. [2020] describe an Early Eocene narrow rift followed by a Late Eocene wide rift governed by detachment faults (Figure 10). (2) Suo et al. [2020] also suggest that the East China Sea Basin (ECSB) located several hundred kilometers to the northeast, recorded a similar evolution in relation to hot asthenospheric flows (Figure 10). (3) South West of the PRMB, the Qiongdongnan basin (QDNB) was affected by an uplift of approximatively 1 km from 30 Ma to 25 Ma [Xie et al., 2006, Zhao et al., 2021] with a lack of compressional deformation [Clift and Sun, 2006]. Here, intraplate volcanism was emplaced synchronously during the uplift event [e.g. Brown et al., 2022]. During this period, local narrow to wide rift-related basins developed, concentrating syn-extension sediments (Figure 10) [Clift and Sun,

2006, Wang et al., 2021]. (4) Northward, the South China Block (SCB) experienced a Miocene km-scale uplift inducing a regional erosional event at this time [Cullen et al., 2010, Morley, 2016, Pubellier and Morley, 2014, Wang et al., 2017, Li and Zou, 2017, Wang et al., 2021, Yan, Y. et al., 2018]. Similarly to other regions, this uplift is associated with intraplate alkaline volcanism and is interpreted as a consequence of hot asthenospheric flow below the SCB. (5) The multistage extension event evidenced in this region was also revealed at the scale of the South China Sea by apatite fission track studies [Wang et al., 2022]. The thermal history modeling reveals successive cooling stages: a rapid cooling process during ca. 80–50 Ma, a slow cooling process during ca. 50–35 Ma and another rapid cooling process during ca. 35–12 Ma. The slow cooling stage can be linked to the subduction of the Izanagi–Pacific spreading ridge [Wang et al., 2022].

Based on Pacific plate kinematic reconstructions, Müller et al. [2008] propose an interpretation of the interaction of the IPR with the South Asian margin, showing a mega-ridge subduction between 70 and 50 Ma (Figure 10). We saw that the main event recorded in the upper plate continental region in response to this kinematic event corresponds to local and regional dynamic uplift associated with OIB volcanism. In addition, extensional deformation across the entire region is responsible for major rift-related basin opening, testifying for tectonic subsidence from Eocene to Late Oligocene times (Figure 10). At a large scale, the stratigraphic records indicate a Late Eocene–Oligocene N–S regional scale uplift up to 3,000,000 km^2 affecting Eastern China and the northern margin of China Sea [Brown et al., 2022] with westward migration towards the South China Block during the Miocene. In addition, OIB magmatism observed from Indochina to the South China Block and extending northward to China and Korea, illustrates the prominant role of asthenospheric flows during Cenozoic times (Figure 10).

To sum up, we may conclude that at 60 Ma, the IPR subducted with a low angle beneath the continental Asia upper plate leading to the progressive development of a large slab-window beneath the South East Asian margin (Figure 10). This large window probably served as a major pathway for Pacific asthenosphere to flow beneath the entire East Asia during Middle to Late Cenozoic [Brown et al., 2022]. Today,

there is no evidence of the 3D geometry of this window, nevertheless as reported above, recent geophysical studies indicate abnormal hot asthenopheric mantle below the upper plate [Zhao et al., 2021]. We are well aware that the Late Cenozoic to Quaternary regional deformations across the South East Asian margin can be attributed to additional subduction processes such as trench retreat and slab roll-back with far-field consequences of the Indian collision. However, based on this review, we may claim that correlations between uplift, intraplate volcanism and extensional deformation above the IPR slab-window during Cenozoic times can be attempted.

5.2.4. *Japan*

Along the Eurasian margin, the Japanese Islands and associated southern Russian Far East (RFE) represent a well-preserved testimony of subduction history since Mesozoic times [e.g. Müller et al., 2016]. The Japan and the Kuril basins located northeast of the Japan islands are currently concerned by the subduction of the Pacific plate whereas the Okinawa and South China basins located south of Japan are concerned by the subduction of the Philippine Sea plate. This was not the case at the beginning of the Cenozoic when most of the margin was affected by the subduction of the Izanagi and Pacific plates (Figure 10), before the growing up of the Philippine Sea plate at 50 Ma [Lallemand, 2016, Liu et al., 2022, Wang et al., 2022, Wu and Wu, 2019].

During Late Jurassic–Cretaceous times, the Japanese Islands were characterized by an Andean-type cordillera where distributed igneous rocks and accretionary prisms developed in relation with subduction processes [Taira et al., 2016, Wakita et al., 2013]. The Japan Sea opened in the Early Miocene in a broad pull-apart zone between two major NNE–SSW dextral strike-slip shear zones [Jolivet et al., 1994, Lallemand and Jolivet, 1986]. The first one extends from north Sakhalin to Central Japan along 2000 km and accommodated 400 km of displacement, the second one, between Korea and SW Japan, accommodates displacement of about 200 km. Here, the extensional domain between these two transcurrent faults forms the back-arc region of Japan with a westward spreading propagation inside the pull-apart region (Figure 10). The basin of the Japan Sea can be viewed first as a back-arc basin opened in relation with the subduction of the Pacific plate [Otofuji et al., 1985,

Uyeda and Kanamori, 1979, Van Horne et al., 2017], but additional processes can be involved, notably because oceanic back-arc spreading is not parallel but orthogonal to the trench direction [Sato, 1994, Yamamoto, 1991]. For some authors [see review in Mantovani et al., 2001] crustal extension occurred in the wake of the Japan arc, which was forced to bend by extrusion between compressional boundaries involving the Okhotsk block and Eurasia. According to Jolivet et al. [1994], internal deformation of Asia due to collision of India has also to be considered. For Tatsumi et al. [1989], the back-arc extension of the Japan Sea occurred between 21 Ma and 14 Ma in response to an asthenospheric injection into the mantle wedge due to a change in the dip of the subduction. Evidence comes from the migration of the arc that can be traced to the surface. During the Oligocene (ca. 30 Ma), the volcanic front was located along the western coast of the present Northeast Japan and migrated about 200 km trenchwards at 23 Ma, before the opening of the Sea of Japan. Therefore, the angle of the subduction became steeper during the period of 30–23 Ma. The Tatsumi et al. [1989]'s model does not involve slab tear nor slab window opening. However, it shows similarities with slab window configuration but upwelling comes from above the slab and does not originate in part from the sub-slab region. The forearc region of northern Japan underwent spectacular tectonic erosion revealed by the subsidence of a regional subaerial unconformity and normal faulting that started 22 Ma ago [Von Huene and Lallemand, 1989].

Interaction of the IPR with the Japanese margin has been documented for several decades at a regional, in particular along the NE–SW accretionary belt of Shimanto (Figure 10). This accretionary wedge is composed of Cretaceous to Neogene sedimentary, magmatic and metamorphic units that record some typical influences of slab-window related to active spreading ridge subduction. The most spectacular event includes: (1) near-trench MORB-type magmatism, (2) abnormal fore-arc thermal event with OIB volcanism, (3) adakites intrusions, (4) HT-BP metamorphic events, (5) gap in sedimentation along the forearc and, (6) erosion at the trench wedge [Hibbard and Karig, 1990, Iwamori, 2000, Kinoshita, 2002, Maeda and Kagami, 1996, Osozawa, 1992, Sakaguchi, 1999, Wu and Wu, 2019]. From a tectonic point of view, the Shimanto belt is characterized by a progres-

sive switch of deformation, from a Paleocene–Early Eocene compressional stage allowing the growing up and the thickening of the prism, to an erosional stage of the margin followed by the collapse of the prism with extensional faulting [e.g. Iwamori, 2000, Osozawa, 1992, Raimbourg et al., 2013, 2014, 2017, Uehara and Aoya, 2005]. This evolution was principally governed by the subduction of the IPR below the Japanese margin.

Landward from the southern margin of the Japan Sea to the Sakhalin Peninsula (Russian Far East), a compilation of magmatic records from Cretaceous to Eocene times highlights the impact of the IPR subduction and the development of the related slab-window (Figure 10). For instance, Wu and Wu [2019] assign the magmatic gap from 56 to 46 Ma along the NE Asian margin to the IPR subduction. After this hiatus, Late Eocene igneous activities bear a more depleted mantle signature with respect to older rocks, consistent with hot-depleted mantle circulation into the mantle wedge allowed by slab-window [Wu and Wu, 2019]. Dynamic topography effects are also reported in the upper plate. This is the case for the Sangliao basin at the northern margin of the Japan Sea (NE China) where an Early Eocene regional unconformity was identified [Song et al., 2014, Wang et al., 2013]. Apatite fission-track dating also suggests intense uplift related to heat upwelling during Early Cenozoic times, from 65 to 50 Ma, in this region [Pang et al., 2020].

Finally, our compilation of geological data shows that the tectonic and magmatic events affecting the Japan margin during the Cenozoic are globally asynchronous and did not occur during the first stages of the subduction of the IPR (Figure 10). Indeed, dynamic uplift occurred from 65–50 Ma to 45 Ma, the magmatism gap was bracketed between 56 and 46 Ma and depleted mantle-related magmatism was emplaced since from 46 Ma. As shown previously, back-arc basins opening occurred during the Oligocene–Miocene times, but some authors suggest that they may have initiated in the Late Cretaceous–Early Eocene [Schellart and Lister, 2005]. Therefore, back-arc basins appear to be 30–20 Ma younger than the IPR subduction and do not coincide exactly with the initiation of slab-window opening below the region. Such a time offset between ridge subduction and continental lithosphere extension can be interpreted as a late response of a thick Eurasian

lithosphere (Andean-type orogen) at the time of the IPR subduction. The thermal effect of asthenospheric mantle flowing through the IPR slab window may be delayed due to thermal inertia. In some cases, thermal erosion, weakening of the upper plate lithosphere and related extensional deformation could occur some million years after ridge subduction.

5.2.5. *Kuril basin and Okhotsk sea*

The Kuril basin is located in the easternmost part of the Eurasian margin, and opened between 30–26 Ma and 15 Ma north of the Kuril arc, in a triangular domain with one side along the Sakhalin–Hokkaido shear zone [Baranov et al., 2002, Kimura and Tamaki, 1985, 1986]. These mid-Eocene to Early Miocene extensional basins were constrained to open mainly in a North–South direction [Fournier et al., 1994, Schellart et al., 2003, Vaes et al., 2019, Worall et al., 1996]. From the Kuril basins and the Okhotsk Sea to the north, we found no mention that these back-arc basins might have opened in relation to spreading ridge subduction and subsequent slab-window at depth. However, some geological records around the Okhotsk Sea testify for interactions between hot asthenospheric upwelling and the upper plate (Figure 10). The first evidence corresponds to the Eocene OIB to adakite-like signature rocks observed in the region of the Okhotsk Sea [Emelyanova et al., 2020] and also found in the eastern part of Kamchatka Peninsula, northeastern China and Honshu Island in Japan [e.g. Emelyanova and Lelikov, 2016]. For these authors, these magmatic products are the consequence of the uprising of hot mantle through a slab-window related to the break-up of the Pacific plate. From the northeastern China margin to the western margin of Okhotsk Sea, apatite fission-track analysis suggests important reheating of the crust during Late Paleocene to Eocene as a consequence of rapid upwelling of asthenospheric mantle [Pang et al., 2020]. Mid-ocean ridge basaltic (MORB) intrusion into forearc sediments (Figure 10), high heat flow and regional uplift have been also recorded from the region surrounding the Russian Far East [Kimura et al., 2019, Wu and Wu, 2019].

Considering the Pacific plates reconstructions of Müller et al. [2008], the IPR intersected the Kuril trench from 60 to 50 Ma leading to the development of a hypothetic slab-window beneath the entire region (Figure 10). Models of Müller et al.

[2016] and Wu et al. [2022a] also include the complex subduction of the Kula spreading ridge, spatially limited to the northern Russia region during Cretaceous and Early Cenozoic times. Therefore, here again, the Late Cretaceous–Eocene tectono-magmatic evolution of the Asian margin could result from ridge subduction inducing development of one or several slab-window beneath Russian Far East. However, as observed in the Japan region, one must point to a timing offset since the extensional/transtensional events in the Kuril region are 30 Ma younger than the first impact of the IPR in the trench.

Finally, to sum up, we may consider that the NE Asian margin and Russian Far East back-arc basins developed during Oligocene and Miocene times, but extensional/transtensional events localizing narrow to wide rift systems may have initiated earlier during Late Cretaceous/Paleocene times (Figure 10). This implies that back-arc basin openings at the western-northwestern tip of the Pacific rim were roughly synchronous, suggesting a regional rather than a local process. The subduction of the long IPR system, subparallel to the trench, and the related opening of a mega-slab window could be a good candidate for such a regional mechanism. The Late Cretaceous–Eocene initiation of extension in the upper plate could be the result of the direct weakening of the lower crust induced by the uprising of hot materiel through slab window near the trench. Further dynamic uplift and thermal doming followed by alkaline magmatism as well as opening of the back-arc basins during the Neogene could represent the effects of a long-lasting thermal erosion of the regional lithosphere with decreased mantle wedge viscosity, at a much larger scale.

5.2.6. *Sunda-Java*

The Sunda-Java area is part of the Sundaland (including Sumatra, Borneo, Java and Indonesia), a complex domain located to the southern tip of the SE Asian margin. Since the Paleozoic period, Sundaland has been affected by several accretion of terranes from Gondwana and South China [e.g. Hall, 2002]. Along the Sunda-Java margin, Jurassic to Cretaceous subduction complexes including ophiolites and arc-type magmatism illustrate long-lived subduction processes [e.g. Clements and Hall, 2011]. Associated with this magmatism, compression recorded in the upper plate was the main factor of the growing up of

this Andean-type cordillera until 80 Ma [Whittaker et al., 2007, Zahirovic et al., 2014, for references]. This tectono-magmatic evolution ended close to the Late Cretaceous–Paleogene boundary with a drastic change from regional compression to initiation of back-arc opening.

As shown previously in Section 5.2.2, the entire region was subjected to Late Cretaceous initiation of active spreading ridge subduction (Figure 10). The first one is west-verging and involves the IPR subduction, the second one is east-verging and involves the Wharton spreading ridge (Figure 10). The latter interaction is well-documented in plate kinematic reconstructions by Whittaker et al. [2007] who infer subduction of the active Wharton ridge between 70 and 43 Ma. This subduction induced the progressive NW–SE migration of a slab-window from southeastern tip of Java and Sumatra (60–45 Ma) to the Central Sumatra (45–30 Ma) (Figure 10).

Sundaland is characterized by the presence of back-arc basins, most of them having recorded extensional deformation from Early Eocene to Late Oligocene [Hall, 2002, Heine et al., 2004, McCourt et al., 1996]. In addition, to the south, the Java Sea experienced extensional deformation from 60 to 45 Ma, inducing the Makassar back-arc spreading ridge (strait located between Borneo and central Sulawesi) [Letouzey et al., 1990, McCourt et al., 1996]. According to Whittaker et al. [2007], slab-window opening is predicted beneath this region between 70 to 45 Ma with a stationary position and thermal weakening of the upper plate. As a result, decreased mantle wedge viscosity associated with this slab-window exacerbated Palaeogene extension and active rifting in the Java Sea region, and enabled Sumatran continental extension to continue at 50–35 Ma (Figure 10). According to Schellart and Lister [2005], this event was preceded by a regional uplift during the Late Cretaceous–Paleogene. Back-arc spreading opening continued during Middle to Late Cenozoic times in response to advance of the upper plate and to slab roll-back processes. To the northwest, Sumatra area has experienced compressional deformation from 15 Ma to present due to the subduction of high bathymetric reliefs of the inactive Wharton Ridge [Whittaker et al., 2007].

At the scale of Sundaland, analysis of geologic records onland confirms the Late Cretaceous–Paleogene regional uplift event, without evidence of compression nor tectonic thickening [e.g. Clements and Hall, 2011, Hall and Nichols, 2002, Morley, 2016, Pubellier and Morley, 2014, Roberts et al., 2018]. As shown by AFT thermochronology dating, the region comprised between Indochina and Java, (i.e. up to 5,600,000 km^2) recorded a long-wavelength uplift of 600 ± 200 m, inducing a regional sedimentary hiatus, ending close to 50 Ma in southern Sumatra-Java to 37 Ma in Central Java [e.g. Clements and Hall, 2011].

6. Conclusion

The time-space evolution of subduction cordilleras is attributed to a diversity of geodynamic processes acting at convergent margins. Understanding the evolution of overriding plate regime requires deciphering the interaction of various physical parameters [see Heuret et al., 2011, Lallemand et al., 2005, Schellart, 2008, Stern, 2002]. Indeed, the cordilleras are sensitive to the subduction polarity and slab retreat/advance dynamics [Doglioni et al., 1999, 2007]. In the case of slab retreat episodes, asthenospheric mantle upwelling cause dynamic topography [e.g. Husson, 2006]. On the other hand, the switch from Altiplano-like topography to collapsed orogen is closely related to the thermo-mechanical state of the overriding plate [Vanderhaeghe and Duchêne, 2010, Vanderhaeghe and Teyssier, 2001, Vanderhaeghe, 2012, Wang and Currie, 2023] and lateral boundary conditions which might alter the tectonic/gravity force balances [e.g. Vanderhaeghe et al., 2003]. All these characteristics can draw and include themselves in a global orogenic cycle of deformation and magmatism [e.g. DeCelles et al., 2009, Wilson et al., 2005]. Notwithstanding, in this review, we are able to identify the process of active spreading ridge subduction as an important factor controlling the tectonic and magmatic status of the upper plate at convergent margins. Since the early days of the Plate Tectonics theory, it has been recognized that elevated subduction cordilleras develop over young subducting oceanic lithosphere (Chile type subduction). By contrast, continental regions experiencing subduction of old oceanic lithosphere are devoid of high relief cordilleras as examplified by the topography of the Aleutians, Kuril, Japan and Indonesia areas. In this paper, we show that in reality, when looking at subduction boundaries in detail, such correlations between the age of the subducting lithosphere

and the elevation of the continental upper plate suffers from significant exceptions. This singularity is illustrated by the active margin of South America where the lowest elevated segments of the Andean Cordillera are found in Patagonia over very young oceanic lithosphere, including the active spreading Chile Ridge.

Based on the Central Patagonia example, we suggest that the subduction of an active spreading ridge triggers thermal doming followed by crustal extension and attenuation of a former elevated cordillera. In addition, plate reconstruction of the Antarctica–South America connection shows that the subduction of three active spreading ridges in this region induced the attenuation and disruption of a former continuous cordillera and led to oceanic spreading in the Scotia basin during the opening of the Drake Passage. Thus, the concentration of several subducting ridges in a given region largely increases the mechanism of thermal erosion of the continental lithosphere of the upper plate, in turn causing large-scale crustal extension giving place in some cases to oceanic spreading in a back-arc environment.

Large amounts of crustal extension leading to exhumation of metamorphic core complexes are well documented along North America (Basin and Range, Columbia, Alaska). Processes of lithosphere thermal erosion at a regional scale accompanying crustal extension ending by back-arc basin opening are largely distributed in the East Asian region in relation to the subduction of the Izanagi–Pacific and Wharton ridges during the Cenozoic.

Our review of active margins worldwide confirms that a variety of situations of active spreading ridge subduction induces a variety of slab-window opening, with geometry varying from isolated gate to mega-pathway. The impact of hot asthenosphere flowing through these different windows generates thermal erosion of the lithospheric mantle, heating and weakening of the crust and in turn various patterns of extensional structures with narrow orthogonal rift (attenuating the relief), to regional back-arc spreading of the overriding plate (causing the full decay of former cordilleras). Active spreading ridge subduction also impacts the tectonic boundary conditions when the ridge enters the trench. In some cases, plate boundary conditions drastically changed during the Cenozoic with free subduction boundaries related to the development of transcurrent fault systems. Nevertheless, we are well aware that our model of cordillera attenuation is not designed for all cases of ridge subductions and still suffers unexplained situations. Firstly, all active continental margins may have developed without a growing cordillera. This was the case for the Andean margin before the Neogene and probably for Sundaland and Japan in the late Cretaceous where testimonies of a previous elevated cordillera are not reported. Secondly, attenuation of cordillera reliefs by extensional tectonics may occur in relation to processes that do not involve active ridge subduction, such as slab roll-back, slab break-off, and tectonic erosion of the margin. Thirdly, in some regions, we evidenced a 10–30 Myr long time span between the first impact of the ridge at the trench and the initiation of the thermal erosion driving the weakening of the upper plate lithosphere by asthenosphere flows through the opened window. This applies to the East Asian margin where the subduction of the IPR mega-ridge is not followed immediately by large-scale lithosphere extension. The reasons for such delays likely relate to the thermo-mechanical properties of the entire system that need further investigations. Nevertheless, our model of attenuation and decay of subduction cordilleras might explain some aspects of the evolution of numerous convergent margins throughout Earth's history.

Declaration of interests

Acknowledgements

Supplementary data

Supporting information for this article is available on the journal's website under https://doi.org/10.5802/crgeos.250 or from the author.

References

Aguillón-Robles, A., Calmus, T., Benoit, M., Bellon, H., Maury, R. C., Cotten, J., Bourgois, J., and Michaud, F. (2001). Late Miocene adakites and Nb-enriched basalts from Vizcaino Peninsula, Mexico: indicators of East Pacific Rise subduction below southern Baja California. *Geology*, 29, 531–534.

Allmendinger, R. W., Jordan, T. E., Kay, S. M., and Isacks, B. L. (1997). The evolution of the Altiplano-Puna plateau of the central Andes. *Annu. Rev. Earth Planet. Sci.*, 25, 139–174.

Ancellin, M. A., Samaniego, P., Vlastélic, I., Nauret, F., Gannouin, A., and Hidalgo, S. (2017). Across-arc versus along-arc Sr-Nd-Pb isotope variations in the Ecuadorian volcanic arc. *Geochem. Geophys. Geosyst.*, 18, 66–79.

Armijo, R., Lacassin, R., Coudurier-Curveur, A., and Carrizo, D. (2015). Coupled tectonic evolution of Andean orogeny and global climate. *Earth Sci. Rev.*, 143, 1–35.

Atwater, T. (1970). Implications of plate tectonics for the Cenozoic tectonic evolution of Western North America. *Geol. Soc. Am. Bull.*, 81, 3513–3536.

Ávila, P. and Dávila, F. D. (2020). Lithospheric thinning and dynamic uplift effects during slab window formation, Southern Patagonia (45°–55°S). *J. Geodyn.*, 133, article no. 101689.

Ávila, P. and Dávila, F. M. (2018). Heat flow and lithospheric thickness analysis in the Patagonian asthenospheric windows, Southern South America. *Tectonophysics*, 13, 99–107.

Baranov, B., Wong, H. K., Dozorova, K., Karp, B., Ludmann, T., and Karnaukh, V. (2002). Opening geometry of the Kurile Basin (Okhostk Sea), as inferred from structural data. *Isl. Arc*, 11, 206–219.

Barnes, M. A. and Barnes, C. G. (1992). Petrology of late Eocene basaltic lavas at Cascade Head, Oregon Coast Range. *J. Volcanol. Geotherm. Res.*, 52, 157–170.

Bekaert, D. V., Gazel, E., and Turner, S. (2021). High ^{3}He/^{4}He in central Panama reveals a distal connection to the Galapagos plume. *Proc. Natl. Acad. Sci.*, 118, 1–8.

Ben Mansour, W., Wiens, D., Mark, H. F., Russo, R. M., Richter, A., Marderwald, E., and Barrientos, S. (2022). Mantle flow pattern associated with the Patagonian slab window determined from azimuthal anisotropy. *Geophys. Res. Lett.*, 49, 1–10.

Blisniuk, P. M., Stern, L. A., Chamberlain, P., Idleman, B., and Zeitler, P. K. (2005). Climatic and ecologic changes during Miocene surface uplift in the Southern Patagonian Andes. *Earth Planet. Sci. Lett.*, 230, 125–142.

Boschman, L. M. (2021). Andean mountain building since the Late Cretaceous: A paleoelevation reconstruction. *Earth Sci. Rev.*, 220, article no. 103640.

Bourgois, J. and Michaud, F. (2002). Comparison between the Chile and Mexico triple junction areas substantiates slab window development beneath Northwestern Mexico during the past 12–10 Myr. *Earth Planet. Sci. Lett.*, 201, 35–44.

Bradley, D., Kusky, T., Haeussler, P., Goldfarb, R., Miller, M., Dumoulin, J., Nelson, S. T., and Karl, S. (2003). Geological signature of early Tertiary subduction in Alaska. In Sisson, V. B., Roeske, S. M., and Pavlis, T. L., editors, *Geological of a Transpressional Orogen Developed During Ridge-Trench Interaction Along the North Pacific Margin*, Geological Society of America, Special Paper 371, page 31. Geological Society of America, Boulder, Colorado.

Breitsprecher, K., Thorkelson, D., Groome, W. G., and Dostal, J. (2003). Geochemical confirmation of the Kula-Farallon slab window beneath the Pacific Northwest in Eocene time. *Geology*, 31(4), 351–354.

Breitsprecher, K. and Thorkelson, D. J. (2009). Neogene kinematic evolution of the Nazca–Antarctic–Phoenix slab windows beneath Patagonia and the Antarctic Peninsula. *Tectonophysics*, 464, 10–20.

Brown, H., Colli, L., and Bunge, H. P. (2022). Asthenospheric flow through the Izanagi-Pacific slab win-

dow and its influence on the dynamic topography and intraplate volcanism in East Asia. *Front. Earth Sci.*, 10, 1–27.

Buck, W. R. (1991). Modes of continental lithospheric extensions. *J. Geophys. Res. Solid Earth*, 96, 20161–20178.

Burkett, E. R. and Billen, M. I. (2009). Dynamics and implications of slab detachment due to ridge-trench collision. *J. Geophys. Res. Solid Earth*, 114, article no. B12402.

Burton-Johnson, A. and Cullen, A. B. (2022). Continental rifting in the South China Sea through extension and high heat flow: an extended history. *Gondwana Res.*, 120, 235–263.

Calmus, T., Bernet, M., Lugo-Zazueta, R., Hardwick, E., and Mendivil-Quijada, H. (2015). Apatite fission-track thermochronology of Laramide plutonic rocks in Northwestern Mexico: distinguishing Basin and Range extension versus Gulf of California rifting. *Rev. Mex. Cienc. Geol.*, 32(3), 529–541.

Cande, S. C. and Leslie, R. B. (1986). Late Cenozoic tectonics of the southern Chile trench. *J. Geophys. Res.*, 91, 471–496.

Cembrano, J., Lavenu, A., Reynolds, P., Arancibia, G., Lopez, G., and Sanhueza, A. (2002). Late Cenozoic transpressional ductile deformation north of the Nazca-South America-Antarctica triple junction. *Tectonophysics*, 354, 289–314.

Charrier, R., Herail, G., Pinto, L., Garcia, M., Riquelme, R., Farias, M., and Munoz, N. (2013). Cenozoic tectonic evolution in the Central Andes in northern Chile and west central Bolivia: Implications for paleogeographic, magmatic and mountain building evolution. *J. Earth Sci.*, 102(1), 235–264.

Clements, B. and Hall, R. (2011). A record of continental collision and regional sediment flux for the Cretaceous and Paleogene core of SE Asia: implications for early Cenozoic palaeogeography. *J. Geol. Soc. Lond.*, 168, 1187–1200.

Clennett, E. J., Sigloch, K., Mitchell, G., Mihalynuk, M. G., Seton, M., Henderson, M. A., Hosseini, K., Mohammadzaheri, A., Johnston, S. T., and Müller, R. D. (2020). A quantitative tomotectonic plate reconstruction of Western North America and the Eastern Pacific Basin. *Geochem. Geophys. Geosyst.*, 20, 1–25.

Clift, P. D. and Sun, Z. (2006). The sedimentary and tectonic evolution of the Yinggehai-Song Hong basin and the southern Hainan margin, South China Sea: Implications for the Tibetan uplift and monsoon. *J. Geophys. Res. Solid Earth*, 111(B6), 1–28.

Cole, R. B. and Basu, A. R. (1992). Middle Tertiary volcanism during ridge-trench interactions in Western California. *Science*, 258, 793–796.

Cole, R. B., Nelson, S. W., Layer, P. W., and Oswald, P. J. (2006). Eocene volcanism above a depleted mantle slab window in Southern Alaska. *Geol. Soc. Am. Bull.*, 118, 140–158.

Cole, R. B. and Stewart, B. W. (2009). Continental margin volcanism at sites of spreading ridge subduction: Examples from southern Alaska and Western California. *Tectonophysics*, 464, 118–136.

Coney, P. J. and Harms, T. A. (1984). Cordilleran metamorphic core complexes: Cenozoic extensional relics of Mesozoic compression. *Geology*, 12, 550–554.

Coney, P. J. and Reynolds, S. J. (1977). Cordilleran Benioff zones. *Nature*, 270, 403–406.

Coutand, I., Diraison, M., Cobbold, P. R., Gapais, D., Rossello, E., and Miller, M. (1999). Structure and kinematics of a foothills transect, Lago Viedma, southern Andes (49°30'S). *J. Soc. Am. Earth Sci.*, 12, 1–15.

Cullen, A., Reemst, P., Henstra, G., Gozzard, S., and Ray, A. (2010). Rifting of the South China Sea: new perspective. *Pet. Geosci.*, 16, 273–282.

Cullen, A. B. (2010). Transverse segmentation of the Baram-Balabac Basin, NW Borneo: refining the model of Borneo's tectonic evolution. *Pet. Geosci.*, 16, 3–29.

Cunningham, W. D. (1993). Strike-slip faults in the southernmost Andes and the development of the Patagonian orocline. *Tectonics*, 12, 169–186.

Cunningham, W. D. (1995). Orogenesis at the southern tip of the Americas: the structural evolution of the Cordillera Darwin metamorphic complex, southernmost Chile. *Tectonophysics*, 244, 197–229.

Davis, A. S., Snavely Jr., P. D., Gray, L. B., and Minasian, D. L. (1995). *Petrology of the Late Eocene Lavas Erupted in the Forearc of Central Oregon: U.S. Geological Survey Open-File Report*, volume 95.

DeCelles, P. G., Ducea, M. N., Kapp, P., and Zandt, G. (2009). Cyclicity in Cordilleran orogenic systems. *Nat. Geosci.*, 2, 251–257.

DeLong, S. E. and Fox, P. J. (1977). Geological consequences of ridge subduction. In Talwani, M.

and Pitman, W. C., editors, *Island Arcs Deep Sea Trenches and Back-Arc Basins*, Maurice Ewing Series, pages 221–228. American Geophysical Union, Washington, DC.

DeLong, S. E., Schwarz, W. M., and Anderson, R. N. (1979). Thermal effects of ridge subduction? *Earth Planet. Sci. Lett.*, 44, 239–246.

DeMets, C., Gordon, R. G., Argus, D. F., and Stein, S. (1990). Current plate motions. *Geophys. J. Int.*, 101, 425–478.

Dewey, J. F. (1988). Extensional collapse of orogens. *Tectonics*, 7, 1123–1139.

Dickinson, W. R. (1997). Tectonic implications of Cenozoic volcanism in coastal California. *GSA Bull.*, 109, 936–954.

Dickinson, W. R. (2006). Geotectonic evolution of the Great Basin. *Geosphere*, 2, 353–368.

Dickinson, W. R. and Snyder, W. S. (1979). Geometry of triple junctions related to San Andreas transform. *J. Geophys. Res.*, 84, 561–572.

Doglioni, C., Carminati, E., Cuffaro, M., and Scorcca, D. (2007). Subduction kinematics and dynamic constraints. *Earth Sci. Rev.*, 83, 125–175.

Doglioni, C., Harabaglia, P., Merlini, S., Mongelli, F., Peccerillo, A., and Piromallo, C. (1999). Orogens and slabs vs. their direction of subduction. *Earth Sci. Rev.*, 45, 167–208.

D'Orazio, M., Agostini, S., Innocenti, F., Haller, J. J., Manetti, P., and Mazzarini, F. (2001). Slab-window-related magmatism from southernmost South America: the Late Miocene mafic volcanics from the Estancia Glencross Area (52° S, Argentina–Chile). *Lithos*, 57, 67–89.

Eagles, G. (2003). Plate tectonics of the Antarctic-Phoenix plate system since 15 Ma. *Earth Planet. Sci. Lett.*, 88, 289–307.

Eagles, G. and Jokat, W. (2014). Tectonic reconstructions for paleobathymetry in Drake Passage. *Tectonophysics*, 611, 28–50.

Eagles, G., Livermore, R. A., Fairhead, J. D., and Morris, P. (2005). Tectonic evolution of the west Scotia Sea. *J. Geophys. Res.*, 11, article no. B02401.

Eagles, G., Livermore, R. A., and Morris, P. (2006). Small basins in the Scotia Sea: the Eocene Drake Passage gateway. *Earth Planet. Sci. Lett.*, 242, 343–353.

Edwards, B. R. and Russell, J. K. (1999). Northern Cordilleran volcanic province: a northern basin and range. *Geology*, 27, 243–246.

Edwards, B. R. and Russell, J. K. (2000). Distribution, nature, and origin of Neogene–Quaternary magmatism in the northern Cordilleran volcanic province, Canada. *GSA Bull.*, 112, 1280–1295.

Emelyanova, T. A. and Lelikov, E. P. (2016). Geochemistry and petrogenesis of the late Mesozoic-Early Cenozoic volcanic rocks of the Okhostk and Japan marginal seas. *Geochem. Int.*, 54(6), 509–521.

Emelyanova, T. A., Petrishchevesky, A. M., Izosov, A., Lee, N. S., and Pugachev, A. A. (2020). Late Mesozoic-Cenozoic stages of volcanism and geodynamics of the Sea of Japan and Sea of Okhotsk. *Petrology*, 28, 418–430.

Engebretson, D. C., Cox, A., and Gordon, R. G. (1985). *Relative Motions Between Oceanic and Continental Plates in Pacific Basin*. Geological Society of America, Special Paper 206. Geological Society of America, Boulder, Colorado.

Espinoza, F., Morata, D., Plové, M., Lagabrielle, Y., Maury, R. C., De la Rupelle, A., Guivel, C., Cotten, J., Bellon, H., and Suarez, M. (2010). Middle Miocene calc-alkaline volcanism in Central Patagonia (47° S): petrogenesis and implications for slab dynamics. *Andean Geol.*, 37, 300–328.

Espinoza, F., Morata, D., Polvé, M., Lagabrielle, Y., Maury, R. C., Guivel, C., Cotten, J., Bellon, H., and Suarez, M. (2008). Bimodal back-arc alkaline magmatism after ridge subduction. Pliocene felsic rocks from Central Patagonia (47° S). *Lithos*, 101, 191–217.

Farris, D. W. and Paterson, S. R. (2009). Subduction of a segmented ridge along a curved continental margin: variation between the Western and Eastern Sanak-Baranof belt, Southern Alaska. *Tectonophysics*, 464, 100–117.

Faulds, J. E., Geismann, J. W., and Maewer, C. K. (1990). Structural development of a major extensional accommodation zone in the Basin and Range province, Northwestern Arizona and southern Nevada. *Geol. Soc. Am. Mem.*, 176, 37–76.

Faulds, J. E. and Varga, R. J. (1998). The role of accommodation zones and transfer zones in the regional segmentation of extended terranes. In Faulds, J. L. and Stewart, J., editors, *The Regional Segmentation of the Basin and Range Province*, Geological Society of America, Special Paper 323, pages 1–45. Geological Society of America, Boulder, Colorado.

Faure, M., Lin, W., Chu, Y., and Lepvrier, C. (2016). Triassic tectonics of the southern margin of the

South China Block. *C. R. Geosci.*, 348, 5–14.

Fernandes, V. M., Roberts, G. G., White, N., and Whittaker, A. C. (2019). Continental-scale landscape evolution: A history of North American topography. *J. Geophys. Res. Earth Surf.*, 124, 2689–2722.

Ferrari, L., Lopez-Martinez, M., Orozco-Esquivel, T., Bryan, S. E., Duque-Trujillo, J., Londsale, P., and Solari, L. (2013). Late Oligocene to Middle Miocene rifting and synextensional magmatism in the Southwestern Sierra Madre Occidental, Mexico: the beginning of the Gulf of California rift. *Geosphere*, 9, 1161–1200.

Ferrari, L., Valencia-Moreno, M., and Bryan, S. (2006). Magmatism and tectonics of the Sierra Madre Occidental and its relation with the evolution of the Western margin of North America. In *Geology of México: Celebrating the Centenary of the Geological Society of México*, Geological Society of America, Special Paper, 422, pages 1–39. Geological Society of America, Boulder, Colorado.

Fosdick, J. C., Romans, B. W., Fildani, A., Bernhardt, A., Calderon, M., and Graham, S. A. (2011). Kinematic evolution of the Patagonian retroarc fold-and-thrusts belt and Magallanes foreland basin, Chile and Argentina, 51°30'S. *GSA Bull.*, 123, 1679–1698.

Fournier, M., Jolivet, L., Huchon, P., Sergeyev, K. F., and Oscorbin, L. S. (1994). Neogene strike-slip faulting in Sakhalin and Japan Sea opening. *J. Geophys. Res.*, 99, 2701–2725.

Fuston, S. and Wu, J. (2020). Raising the Resurrection plate from an unfolded-slab plate tectonic reconstruction of the Northwestern North America since the early Cenozoic time. *GSA Today*, 133(5–6), 1128–1140.

Fyhn, M. B. W., Boldreel, L. O., and Nielsen, L. H. (2009). Geological development of the Central South Vietnamese margin: implications for the establishment of the South China Sea, Indochinese escape tectonics and Cenozoic volcanism. *Tectonophysics*, 478, 184–214.

Garfunkel, Z., Anderson, C. A., and Schubert, G. (1986). Mantle circulation and the lateral migration of subducted slabs. *J. Geophys. Res.*, 91, 4425–4432.

Georgieva, V., Gallagher, K., Sobczyk, A., Sobel, E. R., Schildgen, T. F., Ehlers, T. A., and Strecker, M. R. (2019). Effects of slab-window, alkaline volcanism, and glaciation on thermochronometer cooling histories, Patagonian Andes. *Earth Planet. Sci. Lett.*, 511, 164–176.

Georgieva, V., Melnick, D., Schildgen, T. F., Ehlers, T. A., Lagabrielle, Y., Enkelmann, E., and Strecker, M. R. (2016). Tectonic control on rock uplift, exhumation, and topography above an oceanic ridge collision: Southern Patagonian Andes (47° S), Chile. *Tectonics*, 35(6), 1317–1341.

Gerbault, M., Martinod, J., and Hérail, G. (2005). Possible orogeny-parallel lower crustal flow and thickening in the Central Andes. *Tectonophysics*, 399, 59–72.

Ghiglione, M. C. (2016). Orogenic growth of the Fuegian Andes (52–56° S) and their relation to tectonics of the Scotia Arc. In Folguera, A. et al., editors, *Growth of the Southern Andes*, pages 241–267. Springer Earth System Sciences, Switzerland.

Ghiglione, M. C. and Ramos, V. (2005). Chronology of deformation in the Southernmost Andes of Tierra del Fuego. *Tectonophysics*, 405, 25–46.

Ghiglione, M. C., Ramos, V. A., Cuitino, J., and Barberon, V. (2016). Growth of the Southern Patagonian Andes (46–53° S) and their relation to subduction processes. In Folguera, A. et al., editors, *Growth of the Southern Andes*, pages 201–240. Springer Earth System Sciences, Switzerland.

Gorring, M., Kay, S., Zeitler, P., Ramos, V., Rubiolo, D., Fernandez, M., and Panza, J. (1997). Neogene Patagonian plateau lavas: continental magmas associated with ridge collision at the Chile Triple Junction. *Tectonics*, 16, 1–17.

Gorring, M., Singer, B., Gowers, J., and Kay, S. (2003). Plio-Pleistocene basalts from the Meseta del Lago Buenos Aires, Argentina: evidence for asthenosphere-lithosphere interactions during slab-window magmatism. *Chem. Geol.*, 193, 213–235.

Gorring, M. L. and Kay, S. (2001). Mantle processes and sources of Neogene slab window magmas from Southern Patagonia, Argentina. *J. Pet.*, 42, 1067–1094.

Gregory-Wodzicki, K. (2000). Uplift history of the Central and Northern Andes: a review. *GSA Bull.*, 112, 1091–1105.

Groome, W. G. and Thorkelson, D. J. (2009). The three-dimensional thermo-mechanical signature of ridge subduction and slab window migration. *Tectonophysics*, 464, 70–83.

Groome, W. G., Thorkelson, D. J., Friedman, R. M., Mortensen, J. K., Massey, N. W. D., Marshall, D. D.,

and Layer, P. W. (2003). Magmatic and tectonic history of the Leech River Complex, Vancouver Island, British Columbia: evidence for ridge-trench intersection and accretion of the Crescent Terrane. In Sisson, V. B., Roeske, S. M., and Pavlis, T. L., editors, *Geological of a Transpressional Orogen Developed During Ridge-Trench Interaction Along the North Pacific Margin*, Geological Society of America, Special Paper 371, pages 327–353. Geological Society of America, Boulder, Colorado.

Guillaume, B., Gautheron, C., Simon-Labric, T., Martinod, J., Roddaz, M., and Douville, E. (2013). Dynamic topography control on Patagonian relief evolution as inferred from low temperature thermochronology. *Earth Planet. Sci. Lett.*, 364, 157–167.

Guillaume, B., Martinod, J., Husson, L., Roddaz, M., and Riquelme, R. (2009). Neogene uplift of central Patagonia: dynamic response to active spreading ridge subduction. *Tectonics*, 28, 1–19.

Guillaume, B., Moroni, M., Funiciello, F., Martinod, J., and Faccenna, C. (2010). Mantle flow and dynamic topography associated with slab window opening: Insights from laboratory models. *Tectonophysics*, 496(1–4), 83–98.

Guivel, C., Morata, D., Pelleter, E., Espinoza, F., Maury, R. C., Lagabrielle, Y., Polvé, M., Bellon, H., Cotten, J., Benoit, M., Suarez, M., and De la Cruz, R. (2006). Miocene to Quaternary Patagonia basalts (46–47° S): Geochronometric and geochemical evidence for slab tearing due to active spreading ridge subduction. *J. Volcanol. Geotherm. Res.*, 149, 346–370.

Hall, R. (2002). Cenozoic geological and plate tectonic evolution of the SE Asia and the SW Pacific: computer-based reconstructions, model and animations. *J. Asian Earth Sci.*, 20, 353–434.

Hall, R. and Nichols, G. (2002). Cenozoic sedimentation and tectonics in Borneo: climatic influences on orogenesis. In Jones, S. J. and Frostick, L., editors, *Sediment Flux to Basin: Causes, Controls and Consequences*, Geological Society, London, Special Publication 191, pages 5–22. Geological Society of London.

Hamilton, T. S. and Dostal, J. (2001). Melting of heterogeneous mantle in a slab window environment; examples from the middle Tertiary Masset basalts, Queen Charlotte Islands, British Columbia. *Can. J. Earth Sci.*, 38, 825–838.

Harder, M. and Russell, J. K. (2006). Thermal state of the upper mantle beneath the Northern Cordilleran Volcanic Province (NCVP), British Columbia, Canada. *Lithos*, 87, 1–22.

Heine, C., Müller, R. D., Gaina, C., and Clift, P. (2004). Reconstructing the lost eastern Tethys ocean basin: convergence history of the SE Asian margin and marine gateways. Continent-Ocean interactions within East Asian marginal seas. *Geophys. Monogr. Serv.*, 149, 37–54.

Hell (1977). Tectonic evolution of the Cocos-Nazca spreading center. *GSA Bull.*, 88, 1404–1420.

Heuret, A. and Lallemand, S. (2005). Plate motions, slab dynamics and backarc deformation. *Phys. Earth Planet. Inter.*, 149, 31–51.

Heuret, A., Lallemand, S., Funiciello, F., Piromallo, C., and Faccenna, C. (2011). Physical properties of subduction-type seismogenic zones revisited. *Geochem. Geophys. Geosyst.*, 12, article no. Q01004.

Hibbard, J. P. and Karig, D. E. (1990). Structural and magmatic responses to spreading ridge subduction: an example from southwest Japan. *Tectonics*, 9, 207–230.

Hoggard, M. J., Austermann, J., Randel, C., and Stephenson, S. (2021). Observational estimates of dynamic topography through space and time. In *Mantle Convection and Surface Expressions*, pages 371–411.

Hoggard, M. J., Winterbourne, J., Carnota, K., and White, N. (2017). Oceanic residual depth measurements, the plate cooling model and global dynamic topography. *J. Geophys. Res. Solid Earth*, 122, 2328–2372.

Horton, B. K. (2005). Revised deformation history of the central Andes: inferences from Cenozoic foredeep and intermontane basins of the Eastern Cordillera, Bolivia. *Tectonics*, 24, article no. TC3011.

Horton, B. K. (2018). Tectonic regimes of the Central and Southern Andes: responses to variations on plate coupling during subduction. *Tectonics*, 27, 402–429.

Husson, L. (2006). Dynamic topography above retreating subduction zones. *Geology*, 34(9), 741–744.

Husson, L. (2012). Trench migration and upper plate strain over a convecting mantle. *Phys. Earth Planet. Inter.*, 212–213, 32–43.

Husson, L. and Sempere, T. (2003). Thickening the Altiplano crust by gravity-driven crustal channel

flow. *Geophys. Res. Lett.*, 30, article no. 1243.

Isacks, B. L. (1988). Uplift of the central Andean plateau and bending of the Bolivian orocline. *J. Geophys. Res. Solid Earth*, 93, 3211–3231.

Iwamori, H. (2000). Thermal effects of ridge subduction and its implications for the origin of granitic batholith and paired metamorphic belts. *Earth Planet. Sci. Lett.*, 181, 131–144.

Jarrard, R. D. (1986). Relations among subduction parameters. *Rev. Geophys.*, 24, 217–284.

Jicha, B. R., Singer, B. S., Brophy, J. G., Fournelle, J. H., Johnson, C. M., Beard, B. L., Lapen, T. L., and Mahlen, N. J. (2004). Variable impact of the subducted slab on Aleutian island arc magma sources: evidence from Sr, Nd, Pb, and Hf isotopes and trace element abundances. *J. Pet.*, 45, 1845–1875.

Johnston, S. T. and Thorkelson, D. J. (1997). Cocos-Nazca slab window beneath Central America. *Earth Planet. Sci. Lett.*, 146, 465–474.

Jolivet, L., Tamaki, K., and Fournier, M. (1994). Japan Sea, opening history and mechanism: a synthesis. *J. Geophys. Res. Solid Earth*, 99, 22237–22259.

Jordan, T. E., Isacks, B. L., Allmendinger, R. W., Brewer, J. A., Ramos, V. A., and Ando, C. J. (1983). Andean tectonics related to geometry of subducted Nazca plate. *GSA Bull.*, 94, 341–361.

Jordon, T. E., Nester, P. L., Blanco, N., Hoke, G. D., Davila, F., and Tomlinson, A. J. (2010). Uplift of the Altiplano-Puna plateau: a view from the west. *Tectonics*, 29, 1–31.

Keith, S. (1978). Paleosubduction geometries inferred from Cretaceous and Tertiary magmatic patterns in Southwestern North America. *Geology*, 6, 516–521.

Kimura, G., Kitamura, Y., Yamaguchi, A., Kameda, J., Hashimoto, Y., and Hamahashi, M. (2019). Origin of the early Cenozoic belt boundary thrust and Izinagi-Pacific ridge subduction in the Western Pacific margin. *Isl. Arc*, 28, 1–15.

Kimura, G. and Tamaki, K. (1985). Tectonic framework of the Kuril arc since its initiation. In Nasu, N. et al., editors, *Formation of Active Ocean Margins*, pages 641–676. Springer, Dordrecht.

Kimura, G. and Tamaki, K. (1986). Collision, rotation and back arc spreading. The case of the Okhotsk and Japan seas. *Tectonics*, 5, 389–401.

Kinoshita, O. (2002). Possible manifestation of a slab window magmatism in Cretaceous southwest Japan. *Tectonophysics*, 344, 1–13.

Király, Á., Faccenna, C., and Funiciello, F. (2018). Sub-

duction zones interaction around the Adria microplate and the origin of the Apenninic arc. *Tectonics*, 37, 3941–3953.

Király, A., Portner, D. E., Haynie, K. L., et al. (2020). The effect of slab gaps on subduction dynamics and mantle upwelling. *Tectonophysics*, 785, article no. 228458.

Kistler, R. W. and Peterman, Z. E. (1973). Variations in Sr, Rb, K, Na, and initial Sr87/86Sr in Mesozoic granitic rocks and intruded wall rocks in Central California. *GSA Bull.*, 84, 3482–3512.

Klölcling, M., White, N. J., Maclennan, J., McKenzie, D., and Fitton, J. G. (2018). Quantitative relationships between basalt geochemistry, shear wave velocity, and asthenospheric temperature beneath Western North America. *Geochem. Geophys. Geosyst.*, 19, 3376–3404.

Kraemer, P. E. (2003). Orogenic shortening and the origin of the Patagonian orocline (56 S lat). *J. Soc. Am. Earth Sci.*, 15, 731–748.

Kusky, T. M., Bradley, D. W., and Haeussler, P. (1997). Progressive deformation of the Chugach accretionary complex, Alaska, during a Paleogene ridge-trench encounter. *J. Struct. Geol.*, 19, 139–157.

Lagabrielle, Y., Godderis, Y., Donnadieu, Y., Malavieille, J., and Suarez, M. (2009). The tectonic history of Drake Passage and its possible impacts on global climate. *Earth Planet. Sci. Lett.*, 279, 197–211.

Lagabrielle, Y., Scalabrino, B., Suarez, M., and Ritz, J. F. (2010). Mio-Pliocene glaciations of Central Patagonia: New evidence and tectonic implications. *Andean Geol.*, 37(2), 276–299.

Lagabrielle, Y., Suarez, M., Rossello, E. A., Hérail, G., Martinod, J., Régnier, M., and de la Cruz, R. (2004). Neogene to Quaternary tectonic evolution of the Patagonian Andes at the latitude of the Chile Triple Junction. *Tectonophysics*, 385, 211–241.

Lallemand, S. (2016). Philippine Sea Plate inception, evolution, and consumption with special emphasis on the early stages of Izu-Bonin-Mariana subduction. *Prog. Earth Planet. Sci.*, 3, article no. 15.

Lallemand, S., Heuret, A., and Boutellier, D. (2005). absolute motion, and crustal nature in subduction zones. *Geochem. Geophys. Geosyst.*, 6, article no. Q09006.

Lallemand, S. and Jolivet, L. (1986). Japan Sea: a pull-apart basin? *Earth Planet. Sci. Lett.*, 76, 375–389.

Lamb, S., Hoke, L., Kennan, L., and Dewey, J. (1997).

Cenozoic evolution of the Central Andes in Bolivia and northern Chile. In Burg, J. P. and Ford, M., editors, *Orogeny Through Time*, Geological Society, London, Special Publication 121, pages 237–264. Geological Society of London.

Leeman, W. P., Oldow, J. S., and Hart, W. K. (1992). Lithosphere-scale thrusting in the Western U.S. Cordillera as constrained by Sr and Nd isotopic transitions in Neogene volcanic rocks. *Geology*, 20, 63–66.

Letouzey, J., Werner, P., and Marty, A. (1990). Fault reactivation and structural inversion. Backarc and intraplate compressive deformations. Example of the eastern Sunda shelf (Indonesia). *Tectonophysics*, 183, 341–362.

Lewandowski, W., Jones, C. H., Butcher, L. A., and Maha, K. H. (2018). Lithospheric density models reveal evidence for Cenozoic uplift of the Colorado Plateau and Great Plains by lower-crustal hydratation. *Geosphere*, 14(3), 1–15.

Li, X. and Zou, H. (2017). Late Cretaceous-Cenozoic exhumation of the southeastern margin of coastal mountains, SE China, revealed by fission-track thermochronology: implications for the topographic evolution. *Solid Earth Sci.*, 2, 79–88.

Liu, Y., Liu, L., Li, Y., Peng, D., Wu, Z., Cao, Z., Li, S., and Du, Q. (2022). Global back-arc extension due to trench-parallel mid-ocean ridge subduction. *Earth Planet. Sci. Lett.*, 600, article no. 117889.

Livermore, R., Hillenbrand, C. D., Meredith, M., and Eagles, G. (2007). Drake Passage and Cenozoic climate: an open and shut case. *Geochem. Geophys. Geosyst.*, 8, article no. Q01005.

Livermore, R., Nankivell, A., Eagles, G., and Morris, P. (2005). Paleogene opening of Drake Passage. *Earth Planet. Sci. Lett.*, 236, 459–470.

Londsale, P. (2005). Creation of the Cocos and Nazca plates by fission of the Farallon plate. *Tectonophysics*, 404, 237–264.

Madsen, J. K., Thorkelson, D. J., Friedman, R. M., and Marshall, D. D. (2006). Cenozoic to recent plate configurations in the Pacific Basin: ridge subduction and slab window magmatism in Western North America. *Geosphere*, 1, 11–34.

Maeda, J. and Kagami, H. (1996). Interaction of a spreading ridge and a accretionary prism: implication from MORB magmatism in the Hidaka magmatic zone. *Geology*, 24, 31–34.

Malavieille, J. (1987). Late orogenic extension on mountain belts: insights from the Basin and Range and the late Paleozoic Variscan belt. *Tectonics*, 12(5), 1115–1130.

Mantovani, E., Viti, M., Babbucci, D., Tamburelli, C., and Albarello, D. (2001). Back arc extension: which driving mechanism? *J. Virtual Explor.*, 3, 17–44. General Contributions: 2002.

Mark, C., Chew, D., and Gupta, S. (2017). Does slab-window opening cause uplift of the overriding plate? A case of study from the Gulf of California. *Tectonophysics*, 719–710, 162–175.

Maruyama, S., Isozaki, Y., Kimura, G., and Terabayashi, M. (1997). Paleogeographic maps of Japanese Islands: plate tectonic synthesis form 750 Ma to the present. *Isl. Arc*, 6(1), 121–142.

McCourt, W. J., Crow, M. J., Cobbing, E. J., and Amin, T. C. (1996). Mesozoic and Cenozoic plutonic evolution of SE Asia: evidence from Sumatra, Indonesia. In Hall, R. and Blundell, D., editors, *Tectonic Evolution of Southeast Asia*, Geological Society, London, Special Publications 1006, pages 321–335. Geological Society of London.

Mercer, J. H. and Sutter, J. F. (1982). Late Miocene–earliest Pliocene glaciation in Southern Argentina: implications for global ice-sheet history. *Paleogeogr. Paleoclimatol. Paleoecol.*, 38, 185–206.

Michaud, F., Royer, J. Y., Bourgois, J., Dyment, J., Calmus, T., Bandy, W., Sosson, M., Mortera-Gutiérrez, S. B., Rebolledo-Viera, M., and Pontoise, B. (2006). Oceanic-ridge subduction vs. slab break off: Plate tectonic evolution along the Baja California Sur continental margin since 15 Ma. *Geology*, 34(1), 13–16.

Morell, K. (2015). Late Miocene to recent plate tectonic history of the southern Central America convergent margin. *Geochem. Geophys. Geosyst.*, 16, 3362–3382.

Morley, C. K. (2016). Major unconformities/terminaison of extension events and associated surfaces in the South China Seas: review and implications for tectonic development. *J. Asian Earth Sci.*, 120, 62–86.

Müller, R. D., Sdrolias, M., Gaina, C., Steinberger, B., and Heine, C. (2008). Long-term sea-level fluctuations driven by ocean basin dynamics. *Science*, 319, 1357–1362.

Müller, R. D., Seton, M., Zahirovic, S., Williams, S. E., Matthews, K. J., Wright, N. M., Shepard, G. E., Maloney, K. T., Barnett-Moore, N., Hosseinpour,

M., Bower, D. J., and Cannon, J. (2016). Ocean basin evolution and global-scale plate reorganization events since the Pangea breakup. *Annu. Rev. Earth Planet. Sci.*, 44, 107–138.

Müller, V. A., Calderon, M., Fosdick, J. C., Ghiglione, M. C., Cury, L. F., Massonne, H.-S., Fanning, C. M., Warren, C. J., Arellano, C. R., and Sternai, P. (2021). The closure of the Rocas Verdes basin and early tectono-metamorphic evolution of the Magallanes fold-and-thrust belt, southern Patagonian Andes (52–54° S). *Tectonophysics*, 798, article no. 228686.

Oncken, O., Hindle, D., Kley, J., Elger, K., Victor, P., and Schemmann, K. (2006). Deformation of the Central Andean upper plate system- Facts, Fiction and Constraints for the plateau models. In Oncken, O. et al., editors, *The Andes, Frontiers in Earth Sciences*, pages 3–27. Springer, Berlin, Heidelberg.

Osozawa, S. (1992). Double subduction recorded in the Shimanto accretionary complex, Japan, and plate reconstruction. *Geology*, 20, 939–942.

Otofuji, Y., Matsuda, T., and Nohda, S. (1985). Paleomagnetic evidences for the Miocene counterclockwise rotation of northeast Japan. Rifting process of the Japan arc. *Earth Planet. Sci. Lett.*, 75, 265–277.

Pang, Y., Guo, X., Zhang, X., Zhu, X., Hou, F., Wen, Z., and Han, Z. (2020). Late Mesozoic and Cenozoic tectono-thermal history and geodynamic implications of te Great Xing'an Range, NE China. *J. Asian Earth Sci.*, 189, 104–155.

Pardo-Casas, F. and Molnar, P. (1987). Relative motion of the Nazca (Farallon) and South America plates since Late Cretaceous time. *Tectonics*, 6, 233–248.

Park, C. H., Tamaki, K., and Kobayashi, K. (1990). Age-depth correlation of the Philippine Sea back arc basins and other marginal basins in the world. *Tectonophysics*, 81, 351–371.

Parrish, R. R., Carr, S. D., and Parkinson, D. L. (1988). Eocene extensional tectonics and geochronology of the southern Omineca belt, British Columbia and Washington. *Tectonics*, 7, 181–212.

Pavlis, T. L. and Sisson, V. B. (1995). Structural history of the Chugach metamorphic complex in the Tarra River region, eastern Alaska: a record of Eocene ridge subduction. *GSA Bull.*, 107, 1333–1355.

Pérez-Campos, X., Kim, Y. H., Husker, A., Davis, P. M., Clayton, R. W., Iglesias, A., Pacheco, J. F., Singh, S. K., Manea, V. C., and Gurnis, M. (2008). Horizontal subduction and truncation of the Cocos Plate beneath central Mexico. *Geophys. Res. Lett.*, 35, 1–6.

Perkins, J. P., Ward, K. M., De Silva, S., Zandt, G., Beck, S. L., and Finnegan, N. J. (2016). Surface uplift in the central Andes driven by growth of the Altiplano Puna magma body. *Nat. Commun.*, 7, article no. 13185.

Pubellier, M. and Morley, C. K. (2014). The basins of Sundaland (SE Asia): Evolution and boundary conditions. *Mar. Pet. Geol.*, 58, 555–578.

Raimbourg, H., Augier, R., Famin, V., Gadenne, L., Palazzin, G., Yamaguchi, A., and Kimura, G. (2013). Long-term evolution of an accretionary prism: the case study of the Shimanto belt, Kyushu, Japan. *Tectonics*, 33, 1–24.

Raimbourg, H., Augier, R., Famin, V., Gadenne, L., Palazzin, G., Yamaguchi, A., and Kimura, G. (2014). Long-term evolution of an accretionary prism: the case study of the Shimanto Belt, Kyushu, Japan. *Tectonics*, 33, 1–24.

Raimbourg, H., Famin, V., Palazzin, G., Sakaguchi, A., Yamaguchi, A., and Augier, R. (2017). Tertiary evolution of the Shimanto Belt (Japan); a large-scale collision in early Miocene. *Tectonics*, 36, 1–21.

Ramos, V. and Kay, S. M. (1992). Southern Patagonian plateau basalts and deformation: backarc testimony of ridge collision. *Tectonophysics*, 205, 261–282.

Ramos, V. A. (1989). Andean foothills structures in the northern Magallanes Basin, Argentina. *Am. Assoc. Pet. Geol. Bull.*, 73, 887–903.

Ramos, V. A. (2009). Anatomy and global context of the Andes: Main geologic features and the Andean orogenic cycle. In Kay, S. M. et al., editors, *Backbone of the Americas: Shallow subduction, Plateau Uplift, and Ridge and Terrane Collision*, Memoir 204, pages 31–65. Geological Society of America, Boulder, Colorado.

Ramos, V. A. (2014). An Andean tectonic cycle: From crustal thickening to extension in a thin crust (34°–37° SL). *Geosci. Front.*, 5(3), 351–367.

Reguero, M. A., Goin, F., Acosta, H., Dutra, T., and Marensi, S. (2013). Late Cretaceous/Paleogene West Antarctica Biota and its intercontinental affinities. In Lohmann et al., editors, *South America and the Southern Hemisphere, Dordrecht*, page 120. Springer, Dordrecht, Netherlands.

Rey, P., Vanderhaeghe, O., and Teyssier, C. (2001).

Gravitational collapse of the continental crust: definition, regimes and modes. *Tectonophysics*, 342, 435–449.

Riley, T. R., Milliar, I. L., Carter, A., Flowerdew, M. J., Burton-Johnson, A., Bastias, J., Storey, C. D., Castillo, P, Chew, D., and Whitehouse, M. J. (2023). Evolution of an accretionary complex (LeMay Group) and terrane translation in the Antarctica Peninsula. *Tectonics*, 42, article no. e2022TC007578.

Roberts, G. G., White, N., Hoggard, M. J., Ball, P. W., and Meenan, C. (2018). A Neogene history of mantle convective support beneath Borneo. *Earth Planet. Sci. Lett.*, 496, 142–158.

Roberts, G. G., White, N. J., Martin-Brandis, G. L., and Crosby, A. G. (2012). An uplift history of the Colorado Plateau and its surroundings from inverse modeling of longitudinal river profiles. *Tectonics*, 31, article no. TC4022.

Rogers, R. D., Karason, H., and Van der Hilst, R. D. (2002). Epeirogenic uplift above a detached slab in northern Central America. *Geol. Soc. Am.*, 30, 1031–1034.

Ronda, G., Ghiglione, M. C., Barberon, V., Coutand, I., and Tobal, J. (2019). Mesozoic-Cenozoic evolution of the Southern Patagonian Andes fold and thrust belt (47°–48° S): Influence of the Rocas Verdes basin inversion and onset of Patagonian glaciations. *Tectonophysics*, 765, 83–101.

Russo, R. M. and Silver, P. G. (1994). Trench-parallel flow beneath the Nazca plate from seismic anisotropy. *Science*, 263, 1105–1110.

Russo, R. M. and Silver, P. G. (1996). Cordillera formation, mantle dynamics, and the Wilson cycle. *Geology*, 24, 511–514.

Russo, R. M., Vandecar, J. J., Comte, D., Mocanu, V. I., Gallego, A., and Murdie, R. E. (2010). Subduction of the Chile Ridge: upper mantle structure and flow. *GSA Today*, 20(9), 4–10.

Sakaguchi, A. (1999). Thermal maturity in the Shimanto accretionary prism, southwest Japan, with the thermal change of the subducting slab: fluid inclusion and vitrinite reflectance study. *Earth Planet. Sci. Lett.*, 173, 61–71.

Salze, M., Martinod, J., Guillaume, B., Kermarrec, J. J., Ghiglione, M. C., and Sue, C. (2018). Trench-parallel spreading ridge subduction and its consequences for the geological evolution of the overriding plate: Insights from analogue models and comparison with the Neogene subduction beneath Patagonia. *Tectonophysics*, 737, 27–39.

Sato, H. (1994). The relationship between late Cenozoic tectonic events and stress field and basin development in northeast Japan. *J. Geophys. Res.*, 99, 22261–22274.

Scalabrino, B., Lagabrielle, Y., de la Rupelle, A., Malavieille, J., Polvé, M., Espinoza, F., Morata, D., and Suarez, M. (2009). Subduction of an active spreading ridge beneath Southern South America: A review of the Cenozoic geological records from the Andean foreland, Central Patagonia (46–47° S). In Lallemand and Funiciello, editors, *Subduction Zone Geodynamics*. Springer-Verlag, Heidelberg, Berlin.

Scalabrino, B., Lagabrielle, Y., Malavieille, J., Dominguez, S., Melnick., D., Espinoza, F., Suarez, M., and Rossello, E. (2010). A morphotectonic analysis of Central Patagonian Cordillera. Negative inversion of the Andean belt over a buried spreading center? *Tectonics*, 29, 1–27.

Scalabrino, B., Ritz, J. F., and Lagabrielle, Y. (2011). Relief inversion triggered by subduction of an active spreading ridge: evidence from glacial morphology in Central Patagonia. *Terra Nova*, 23, 63–69.

Schellart, W. P. (2008). Overriding plate shortening and extension above subduction zones: a parametric study to explain formation of the Andes Mountains. *GSA Bull.*, 120, 1441–1454.

Schellart, W. P., Jessel, M. W., and Lister, G. S. (2003). Asymmetric deformation in the backarc region of Kuril arc, northwest Pacific: New insights from analogue modeling. *Tectonics*, 22(5), article no. 1047.

Schellart, W. P. and Lister, G. S. (2005). The role of the East Asian active margin in widespread extensional and strike-slip deformation on East Asia. *J. Geol. Soc. Lond.*, 162, 959–972.

Sdrolias, M. and Müller, D. (2006). Controls on backarc basin formation. *Geochem. Geophys. Geosyst.*, 7, article no. Q04016.

Sempere, T., Butler, R. F., Richards, D. R., Marshall, W., and Swisher, C. C. (1997). Stratigraphy and chronology of Upper Cretaceous-lower Paleogene strata in Bolivia and northwest Argentina. *GSA Bull.*, 109, 709–727.

Sempere, T., Herail, G., Oller, J., and Bonhomme, M. G. (1990). Late Oligocene-early Miocene major tectonic crisis and related basins in Bolivia. *Geol-*

ogy, 18(10), 946–949.

Seton, M., Flament, N., Whittaker, J., Müller, R. D., Gurnis, M., and Bower, D. J. (2015). Ridge subduction sparked reorganization of the Pacific plate-mantle system 60–50 million years ago. *Geophys. Res. Lett.*, 42, 1732–1740.

Seton, M., Müller, R. D., Zahirovic, S., Williams, S., Wright, N. M., Cannon, J., Whittaker, J. M., Matthews, K. J., and McGirr, R. (2020). A global data set of present-day oceanic crustal age and seafloor spreading parameters. *Geochem. Geophys. Geosyst.*, 21, article no. e2020GC009214.

Severinghaus, J. and Atwater, T. (1990). Cenozoic geometry and thermal state of the subducting slabs beneath Western North America. In Wernicke, B. P., editor, *Basin and Range Extensional Tectonics Near the Latitude of Las Vegas, Nevada*, Geological Society of America Memoir, 176. Geological Society of America, Boulder, Colorado.

Shemenda, A. I. (1992). Horizontal lithosphere compression and subduction; constraints provided by physical modelling. *J. Geophys. Res.*, 97, 11097–11116.

Shemenda, A. I. (1994). *Subduction: Insights from Physical Modeling.* Kluwer Academic Publishers, Dordrecht, Netherlands.

Singer, B. S. and Myers, J. D. (1990). Intra-arc extension and magmatic evolution in the Central Aleutian Arc, Alaska. *Geology*, 18, 1050–1053.

Singer, B. S., Myers, J. D., and Frost, C. D. (1992). Mid-Pleistocene lavas from the Seguam volcanic center, central Aleutian arc: closed-system fractional crystallization of a basalt to rhyodacite eruptive suite. *Contrib. Mineral. Petrol.*, 110, 87–112.

Sisson, V. and Pavlis, T. (1993). Geologic consequences of plate reorganization: an example from the Eocene southern Alaska fore arc. *Geology*, 21, 913–916.

Sisson, V. B., Hollister, L. S., and Onstott, T. C. (1989). Petrologic and age constraints on the origin of a low-pressure/high-temperature metamorphic complex, southern Alaska. *J. Geophys. Res.*, 94, 4392–4410.

Sisson, V. B., Pavlis, T. L., Roeske, S. M., and Thorkelson, D. J. (2003). Introduction: An overview of ridge-trench interactions in modern and ancient settings. In Sisson, V. B., Roeske, S. M., and Pavlis, T. L., editors, *Geological of a Transpressional Orogen Developed During Ridge-Trench Interaction Along the North Pacific Margin*, Geological Society of America, Special Paper 371, pages 1–18. Geological Society of America, Boulder, Colorado.

Somoza, R. (1998). Updated Nazca (Farallon) – South American relation motion during the last 40 Ma. Implications for mountain building in the Central Andean region. *J. South Am. Earth Sci.*, 11, 211–215.

Song, Y., Ren, J., Stepashko, A., and Li, J. (2014). Post-rift geodynamics of the Songliao Basin, NE China: Origin and significance of T11 (Coniacian) unconformity. *Tectonophysics*, 634, 1–18.

Stephenson, S. N., Roberst, M. J., Hoggard, A. C., and Whittaker, C. (2014). A Cenozoic uplift history of Mexico and its surroundings form longitudinal river profiles. *Earth Planet. Sci. Lett.*, 519, 61–69.

Stern, R. J. (2002). Subduction zones. *Rev. Geophys.*, 40(4), article no. 1012.

Stevens Godard, A. L. and Fosdick, J. C. (2019). Multichronometer thermochronology modeling of migrating spreading ridge subduction in southern Patagonia. *Geology*, 47, 555–558.

Stewart, J. H. and Roldán-Quintana, J. (1994). *Map showing late Cenozoic extensional tilt patterns and associated structures in Sonora and adjacent areas, Mexico.* US Geological Survey, Map MF-2238.

Stock, J. and Hodges, K. V. (1989). Pre-Pliocene extension around the Gulf of California and the transfer of Baja California to the Pacific Plate. *Tectonics*, 13, 1472–1487.

Suo, Y., Dong, H., Liu, L., Peng, D., Li, Y., Liu, J., Dai, L., Cao, X., and Li, S. (2020). Landward mantle flow associated with the Pacific subduction system opened the South China Sea. *Research Square Open Archive*, 1–22. https://doi.org/10.21203/rs.3.rs-2332418/v1.

Taboada, A., Rivera, L. A., Fuenzalida, A., Cisternas, A., Philip, H., Bijwaard, H., Olaya, J., and Rivera, C. (2000). Geodynamics of the northern Andes: subductions and intracontinental deformation (Colombia). *Tectonics*, 19, 787–813.

Taira, A., Ohara, Y., Wallis, S. R., Ishiwatari, A., and Iryu, Y. (2016). Geological evolution of Japan: an overview. In *The Geology of Japan*. Geological Society of London.

Tatsumi, Y., Otofuji, Y.-O., Matsuda, T., and Nohda, S. (1989). Opening of the Sea of Japan back-arc basin by asthenospheric injection. *Tectonophysics*, 164(4), 317–329.

Thomson, S. N., Brandon, M. T., Tomkin, J. H., Rein-

ers, P. W., Vasquez, C., and Wilson, N. J. (2010). Glaciation as a destructive and constructive control on mountain building. *Nature*, 467, 313–317.

Thomson, S. N., Hervé, F., and Stockhert, B. (2001). Mesozoic-Cenozoic denudation history of the patagonian Andes (Southern Chile) and its correlation to different subduction processes. *Tectonics*, 20, 693–711.

Thorkelson, D. J. (1996). Subduction of diverging plates and the principles of slab window formation. *Tectonophysics*, 255, 47–63.

Thorkelson, D. J., Madsen, J. K., and Sluggett, C. L. (2011). Mantle flow through the Northern Cordilleran slab window revealed by volcanic geochemistry. *Geology*, 39(3), 267–270.

Thorkelson, D. J. and Taylor, R. P. (1989). Cordilleran slab windows. *Geology*, 17, 833–836.

Torsvik, T. H., Steinberger, B., Shepard, G. E., Doubrovine, P. V., Gaina, C., Dormeier, M., Conrad, C. P., and Sager, W. (2019). Pacific-Panthalassic reconstructions: Overview, errata and the way forward. *Geochem. Geophys. Geosyst.*, 20, 3659–3689.

Uehara, S. I. and Aoya, M. (2005). Thermal model for approach of a spreading ridge to subduction zones and its implications for high-P/high-T metamorphism: Importance of subduction versus ridge approach ratio. *Tectonics*, 24, article no. TC4007.

Underwood, M. B., Shelton, K. L., McLaughlin, R. J., Laughland, M. M., and Solomon, R. M. (1999). Middle Miocene anomalies within the Franciscan Complex of Northern California: thermo-tectonic responses near the Mendocino triple junction. *GSA Bull.*, 111, 1448–1467.

Uyeda, S. (1982). Subduction zones: An introduction to comparative subductology. *Tectonophysics*, 81, 133–159.

Uyeda, S. and Kanamori, H. (1979). Back arc opening and the mode of subduction. *J. Geophys. Res. Atm.*, 84, 1049–1061.

Vaes, B., Douwe, J., Hinsberger, J., and Boschman, L. M. (2019). Reconstruction of subduction and back-arc spreading in the NW Pacific and Aleutian Basin: Clues to causes of Cretaceous and Eocene plate reorganizations. *Tectonics*, 38, 1367–1414.

Van Horne, A., Sato, H., and Ishiyama, T. (2017). Evolution of the Sea of Japan back-arc and some unsolved issues. *Tectonophysics*, 710–711, 6–20.

Vanderhaeghe, O. (2012). The thermal-mechanical evolution of the crustal orogenic belts at convergent plate boundaries: A reappraisal of the orogenic cycle. *J. Geodyn.*, 56–57, 124–145.

Vanderhaeghe, O. and Duchêne, S. (2010). Crustal-scale mass transfer, geotherm and topography at convergent plate boundaries: Crustal dynamics at convergent boundaries. *Terra Nova*, 22, 315–323.

Vanderhaeghe, O., Medvedev, S., Fullsack, P., Beaumont, C., and Jamieson, R. A. (2003). Evolution of orogenic wedges and continental plateau: insights from crustal thermal-mechanical models overlying subducting mantle lithosphere. *Geophys. J. Int.*, 153, 27–51.

Vanderhaeghe, O. and Teyssier, C. (2001). Partial melting and flow of orogens. *Tectonophysics*, 342, 451–472.

Varga, R. J., Faulds, J. E., and Harlan, S. (1996). Regional extent and dominant geometry of the Black Mountains accommodation zone, northwest Arizona and southern Nevada. *Geol. Soc. Am. Abstr. Progr.*, 28, 512.

Vérard, C., Flores, K., and Stampfli, G. (2012). Geodynamic reconstructions of the South America–Antarctica plate system. *J. Geodyn.*, 53, 43–60.

Von Huene, R. and Lallemand, S. (1989). Tectonic erosion along the Japan and Peru convergent margins. *Geol. Soc. Am. Bull.*, 102, 704–720.

Wakita, K., Pubellier, M., and Windley, B. F. (2013). Tectonic processes, from rifting to collision via subduction, in SE Asia and the Western Pacific: a key to understanding the architecture of the Central Asian orogenic belt. *Lithos*, 5, 265–276.

Wang, C., Scott, R. W., Wan, X., Graham, S. A., Huang, S. A., Wang, P., Wu, H., Dean, W. E., and Zhang, L. (2013). Late Cretaceous climate changes recorded in eastern Asian lacustrine deposits and North American Epieric sea strata. *Earth Sci. Rev.*, 126, 275–299.

Wang, D. and Shu, L. (2012). Late Mesozoic basin and range tectonics related magmatism in Southeast China. *Geosci. Front.*, 3, 109–124.

Wang, H. and Currie, C. A. (2023). Stepwise widening of the Central Andes – The role of the lower crust. *Geophys. Res. Lett.*, 50, article no. e2023GL103969.

Wang, P., Li, S., Suo, Y., Guo, L., Santosh, M., Li, X., Wang, G., Jiang, Z., Liu, B., Jiang, S., Cao, X., and Liu, Z. (2021). Structural and kinematic analysis of Cenozoic rift basins in South China Sea: a synthesis. *Earth Sci. Rev.*, 216, article no. 103522.

Wang, P., Suo, Y., Cao, X., Zhu, J., Liu, B., Wang,

G., Zhou, G., Li, X., Li, S., and Hui, G. (2022). Late Cretaceous-Cenozoic cooling of the southern Lower Yangtze River area: A response to subduction of the Izanagi and Pacific plates. *Gondwana Res.*, 102, 31–45.

Wang, W., Ye, J., Biggoli, T., Yang, X., Shi, H., and Shu, Y. (2017). Using detrital zircon geochronology to constrain Paleogene provenance and its relationship to rifting in the Zhu 1 depression, Pearl River Mouth Basin, South China Sea. *Geochem. Geophys. Geosyst.*, 18, 3976–3999.

Wernicke, B. P. (1981). Low-angle normal faults in the Basin and Range province—nappe tectonics in an extending orogen. *Nature*, 291, 645–648.

Wernicke, B. P. (1985). Uniform-sense normal simple shear of the continental lithosphere. *Can. J. Earth Sci.*, 22, 108–125.

Wernicke, B. P. (2009). The detachment era (1977–1982) and its role in revolutionizing continental tectonics. In Ring, U. and Wernicke, B., editors, *Extending a Continent: Architecture, Rheology and Heat Budget*, Geological Society, London, Special Publications 321, pages 1–8. Geological Society of London.

Wernicke, B. P., England, P. C., Sonder, L. J., and Christiansen, R. L. (1987). Tectonomagmatic evolution of Cenozoic extension in the North America Cordillera. In Coward, M. P., Dewey, J. F., and Hancock, P. L., editors, *Continental Extensional Tectonics*, Geological Society, London, Special Publication 28. Geological Society of London.

Whittaker, J. M., Müller, R. D., Sdrolias, M., and Heine, C. (2007). Sunda-Java trench kinematics, slab window formation and overriding plate deformation since the Cretaceous. *Earth Planet. Sci. Lett.*, 255, 445–457.

Willett, C. D., Ma, K. F., Brandon, M. T., Hourigan, J. K., Christeleit, E. C., and Shuster, D. L. (2020). Transient glacial incision in the Patagonia Andes from 6 Ma to present. *Sci. Adv.*, 6, 1–9.

Wilson, D. S., McCrory, P. A., and Stanley, R. G. (2005). Implications of volcanism in coastal California for the Neogene deformation history of Western North America. *Tectonics*, 24, article no. TC 3008.

Worall, D. M., Kruglyak, V., Kunst, F., and Kuznetsov, V. (1996). Tertiary tectonics of the Sea of Okhotsk, Russia. Far-field effects of the India-Eurasia collision. *Tectonics*, 15(4), 813–826.

Wu, J., Lin, Y. A., Flament, N., Wu, J. T.-J., and Liu, Y. (2022a). Northwest Pacific-Izanagi plate tectonics since Cretaceous times from Western Pacific mantle structure. *Earth Planet. Sci. Lett.*, 583, article no. 117445.

Wu, J. T.-J. and Wu, J. (2019). Izanagi-Pacific ridge subduction revealed by a 56 to 46 Ma magmatic gap along the northeast Asian margin. *Geology*, 47(10), 953–957.

Wu, Y., Liao, J., Guo, F., Wang, X.-C., and Shen, Y. (2022b). Styles of trench- parallel mid-ocean ridge subduction affect Cenozoic geological evolution in circum-Pacific continental margins. *Geophys. Res. Lett.*, 49, article no. e2022GL098428.

Xie, X., Muller, R. D., Li, S., Gong, Z., and Sterinberger, B. (2006). Origin of the anomalous subsidence along the Northern South China Sea margin and its relationship to dynamic topography. *Mar. Petrol. Geol.*, 23(7), 745–765.

Yamamoto, T. (1991). Late Cenozoic dyke swarms and tectonic stress field in Japan. *Bull. Geol. Surv. Jpn*, 42, 131–148.

Yan, Q., Shi, X., Metcalfe, I., Liu, S., Xu, T., Kornkanitnan, N., Sirichaiseth, T., Yuan, L., Zhang, Y., and Zhang, H. (2018). Hainan mantle plume produced late Cenozoic basaltic rocks in Thailand, Southeast Asia. *Nature*, 8, article no. 2640.

Yan, Y., Yao, D., Tian, Z. X., Huang, C. Y., Dilek, Y., Clift, P. D., and Li, Z. A. (2018). Tectonic topography changes in Cenozoic east Asia: A landscape erosion-sediment archive in the South China Sea. *Geochem. Geophys. Geosyst.*, 19, 1731–1750.

Zahirovic, S., Seton, M., and Müller, R. D. (2014). The Cretaceous and Cenozoic tectonic evolution of Southeast Asia. *Solid Earth*, 5, 227–273.

Zhang, Y., Yao, Y., Li, X., Shang, L., Yang, C., Wang, Z., Wang, M., et al. (2020). Tectonic evolution and resource-environmental effect of China Seas and adjacent areas under the multisphere geodynamic system of the East Asia ocean-continent convergent belt since Mesozoic. *Geol. China*, 47(5), 1271–1309.

Zhao, D., Toyokuni, G., and Kurata, K. (2021). Deep mantle structure and origin of Cenozoic intraplate volcanoes in Indochina, Hainan and South China Sea. *Geophys. J. Int.*, 225(1), 572–588.

Ziagos, J. P., Blackwell, D. D., and Mooser, F. (1985). Heat flow in southern Mexico and the thermal effects of subduction. *J. Geophys. Res. Solid Earth*, 90, 5410–5420.